Advances in Colloid and Interface Science 257 (2018) 1–18

Contents lists available at ScienceDirect

Advances in Colloid and Interface Science

journal homepage: www.elsevier.com/locate/cis

Historical perspective

PAMAM dendrimer - cell membrane interactions

Laura J. Fox [a,b], Robert M. Richardson [c], Wuge H. Briscoe [a,*]

[a] School of Chemistry, University of Bristol, Cantock's Close, Bristol BS8 1TS, United Kingdom
[b] Bristol Centre for Functional Nanomaterials, H.H. Wills Physics Laboratory, Tyndall Avenue, University of Bristol, Bristol BS8 1TL, United Kingdom
[c] School of Physics, H.H. Wills Physics Laboratory, Tyndall Avenue, University of Bristol, Bristol BS8 1TL, United Kingdom

ARTICLE INFO

Available online 27 June 2018

ABSTRACT

PAMAM dendrimers have been conjectured for a wide range of biomedical applications due to their tuneable physicochemical properties. However, their application has been hindered by uncertainties in their cytotoxicity, which is influenced by dendrimer generation (i.e. size and surface group density), surface chemistry, and dosage, as well as cell specificity. In this review, biomedical applications of polyamidoamine (PAMAM) dendrimers and some related cytotoxicity studies are first outlined. Alongside these in vitro experiments, lipid membranes such as supported lipid bilayers (SLBs), liposomes, and Langmuir monolayers have been used as cell membrane models to study PAMAM dendrimer-membrane interactions. Related experimental and theoretical studies are summarized, and the physical insights from these studies are discussed to shed light on the fundamental understanding of PAMAM dendrimer-cell membrane interactions. We conclude with a summary of some questions that call for further investigations.

Contents

* Corresponding author.
E-mail address: wuge.briscoe@bristol.ac.uk (W.H. Briscoe).

https://doi.org/10.1016/j.cis.2018.06.005

1. Introduction

1.1. Application of nanoparticles and nanomaterials

Nanoparticles are increasingly incorporated in modern applications ranging from biosensors [1] to food additives [2], and many fundamental studies have been dedicated to the properties of nanoparticle dispersions [3]. The physicochemical properties of nanoparticles, such as reactivity, melting point and conductivity, are different from those of the bulk material and can be exploited for enhanced product functionality and performance. Concurrently, it also poses profound challenges due to uncertainties associated with the biocompatibility and cytotoxicity of nanoparticles and nanomaterials, particularly in biomedical applications. A key consideration here is related to how nanoparticles and nanomaterials enter cells, either by endocytosis or passive, non-endocytic mechanisms. Endocytosis is any energy dependent uptake mechanism and includes micropinocytosis, clathrin-dependent endocytosis, caveolae and clathrin- and caveolin- independent mechanisms all with different proceeding intracellular pathways [4]. Understanding cellular entry of nanoparticles is also essential to their potential applications such as targeted drug delivery and medical imaging [5]. However, our understanding of cytotoxicity of nanomaterials and nanoparticles, particularly how they impart interactions with cell membranes, remains limited [6].

1.2. Dendritic nanoparticles

Dendrimers are branched polymeric nanoparticles, and have been investigated for a range of biomedical applications [7, 8] such as drug [9] and gene delivery [10], due to the possibility for precise control over their physicochemical properties. Their size, shape and surface charge can be tuned for bypassing the cellular membrane [11, 12], forming complexes with DNA [13, 14], and solubilising hydrophobic drugs [9]. It is this precise control over the physicochemical properties that makes dendrimers unique among other nanoparticles, such as polymer and surfactant micelles [15, 16], also of interest for biomedical applications.

Dendrimers are made up of layers of dendrons (i.e. concentric branching units) radiating from a central initiator core, where each layer is termed a generation (G) [17]. Highly monodisperse dendrimers can be synthesised, and the reactive end groups allow for additional functionality. The choice of the initiator core can also help to determine the dendrimer structure, such as the number of dendron branches and the size and number of the cavities within a dendrimer. There are over 100 families of dendrimer particles with different initiator cores, including carbon, nitrogen and phosphorus, as well as different branching units and multiplicities [18]. A small number of dendrimer products are available on the consumer market, for example VivaGel® which consists of a G4 polylysine dendrimers that is used for bacterial vaginosis treatment and protection against HIV [19].

1.3. PAMAM dendrimers

First reported by Tomalia et al. in the 1980's, PAMAM dendrimers were the first complete family of dendrimers to be synthesised and commercialised and are one of the most studied. The diameter (D) of PAMAM dendrimers ranges from 1 nm to 14 nm (or correspondingly from G0 to G10) measured using TEM, DLS, nanoES-GEMMA (electrospray gas-phase electrophoretic mobility molecular analyser), SAXS and molecular dynamics (MD) simulation, presented in Table 1 [17], as well as their radius of gyration (R_g) and zeta potential (where applicable).

Either ethylenediamine (EDA), ammonia (NH_3) or cystamine is used as the initiator core, providing different numbers of possible branches (multiplicities) as shown in Fig. 1(a). The interior generations are made sequentially from N-(2-aminoethyl) acrylamide via a two-step process. The first step is the addition of methyl acrylate to a core amine group and the second step is amidation of the resulting esters with EDA. Half-generation dendrimers can be made by terminating this process after step 1, resulting in terminal ester groups [25]. The geometrically progressive growth results in the linear increase of the particle diameter at an increment of ~1 nm, an exponential increase in reactive terminal end groups and approximately a doubling of the molecular weight (MW) with each new dendrimer generation. The terminal amine groups can be functionalised in a variety of ways, most commonly with hydroxyl (OH), carboxylic acid (COOH) [26] or conjugation to hydrocarbon chains and PEG [27].

2. Applications of PAMAM dendrimers

2.1. Cargo and drug delivery

In 1990, electron micrographs [28] revealed that some PAMAM dendrimers had hollow cores. Since then, it has been shown that G4-6 PAMAM dendrimers mimic the topology of micelles and their accessible interiors could be used to encapsulate small guest molecules, such as hydrophobic drugs [29]. The open, flexible structure of lower generation dendrimers (G0–3) and the rigid surface of high generation dendrimers due to steric branch crowding (G7–10) provided less efficient encapsulation [30]. Both the core size and surface 'congestion' affected the size of the cargo space, and the encapsulation and release properties could also be tailored depending on the bulk solution conditions such as pH, polarity and temperature [31]. For example, PAMAM has been combined with tris(hydroxymethyl) amino methane (TRIS) to bind various

Table 1
Diameter (D), radius of gyration (R_g) and zeta potential of PAMAM dendrimers (G0–10) measured using DLS, SAXS, nano-ES-GEMMA (electrospray gas-phase electrophoretic mobility molecular analyser), TEM and MD simulations.

Generation	Theoretical no. of NH_2 groups	D (nm)			R_g (nm)		Zeta Potential[b] (mV)
		TEM[a]	DLS[b]	nanoES-GEMMA[c]	SAXS[d]	MD[e]	
0	4					0.493	
1	8					0.746	
2	16			3.3		0.917	
3	32		3.1		1.58	1.123	43.3
4	64		4.2	4.3	1.71	1.45	34.6
5	128	4.3	5.5	5.1	2.41	1.834	43.3
6	256	6.9	7.5	6.4	2.63	2.24	46.2
7	512	8.0		7.6	3.19	2.909	
8	1024				4.03	3.642	
9	2048	12.4		11.2	4.92	4.603	
10	4096	14.7		14.0	5.74	5.519	

[a] [20].
[b] [21].
[c] [22].
[d] [23].
[e] [24].

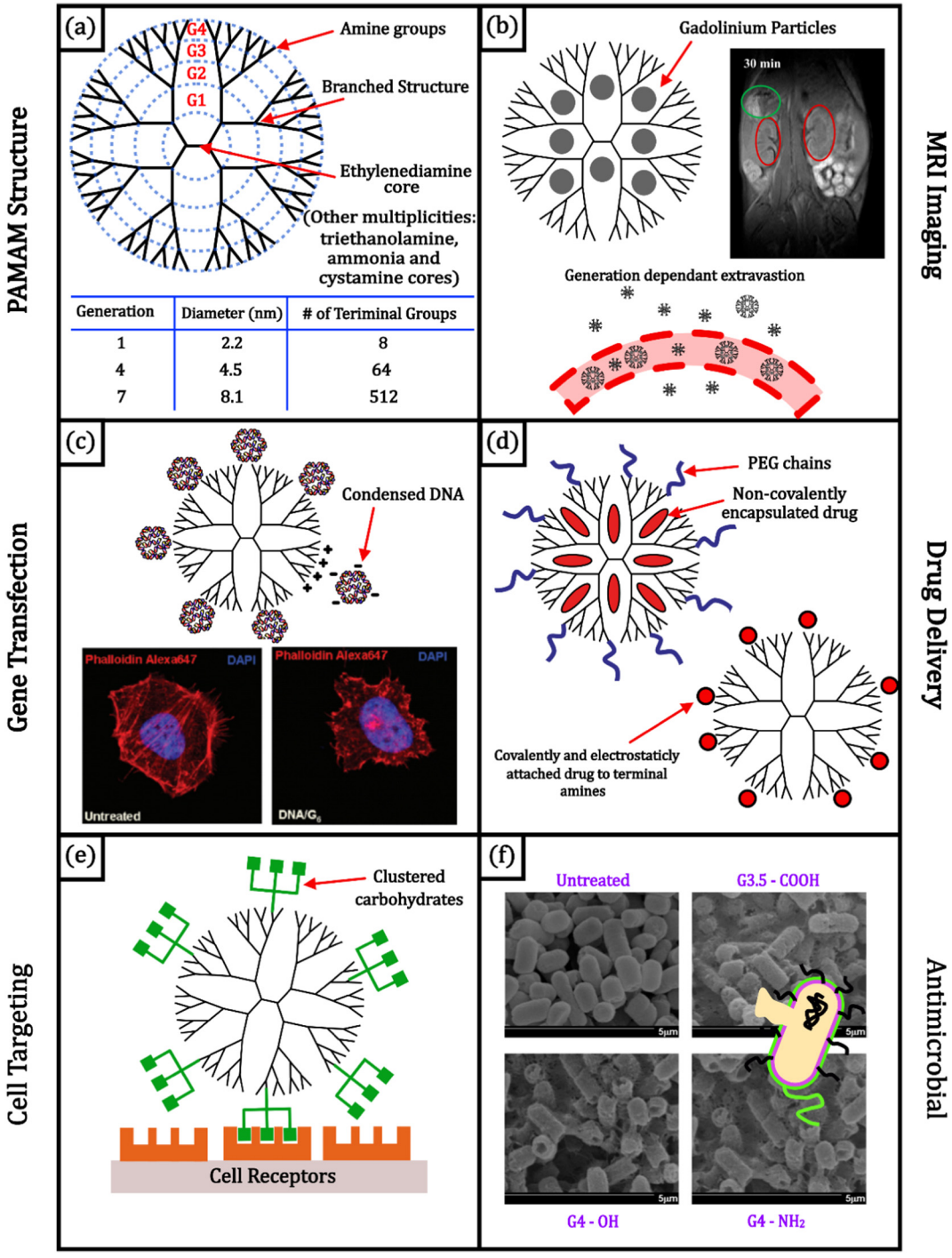

Fig. 1. Biomedical applications of PAMAM dendrimers. (a) The branched structure of PAMAM dendrimers with examples of the size of various generations taken from Porianazar et al. (b) Gadolinium (Gd) particles encapsulated in PAMAM cavities can be used as dual-contrast agents in MRI imaging. The efficiency of PAMAM as MRI agents depends upon the generation of the dendrimer. The MRI image on the right shows darker contrast in the kidneys (red ovals) 30 min after injection of G4.5-Gd conjugates (adapted with permission from [48] Copyright 2017 American Chemical Society). (c) DNA can complex with the positively charged terminal groups on PAMAM which has shown to increase transfection. Confocal images (adapted with permission from [38] Copyright 2011 American Chemical Society) demonstrate the localisation of PAMAM-DNA conjugates in the cell nucleus. (d) PAMAM can be used as drug delivery vehicles by encapsulation of drugs in the interior cavities or covalent/electrostatic attachment of drug molecules to their periphery. PEG functionalisation is found to decrease PAMAM cytotoxicity and increase circulation times, as discussed by Choudhary et al. (e) The functionalisation of PAMAM periphery amine groups with carbohydrates and folates has shown to result in cell-specific targeting, as demonstrated by Bezouška et al. and Konda et al. (f) PAMAM dendrimers with —OH, —COOH and —NH2 terminal groups have demonstrated antimicrobial properties towards *E. coli* resulting in cell lysis as shown in SEM images (adapted with permission from [26]. Copyright 2010 Elsevier).

antibacterial compounds, which could then be released at low pH [32]. In addition to encapsulation in the dendrimer interior, the terminal functional groups at the dendrimer periphery can be used for complexation and conjugation of larger molecules. For instance, drug molecules and targeting moieties have been covalently attached to dendrimer surfaces [29]. The reactive amine groups on the PAMAM dendrimer periphery have also been functionalised with folates [33] and carbohydrates (coined glycodendrimers) [34] for cell specific targeting.

2.2. Gene transfection

Haensler and Szoka reported in 1993 [35] that DNA-PAMAM dendrimer complexes showed high transfection efficiencies for mammalian cells. The most promising complexes were formed with amino-terminated, low generation dendrimers which were thought to enhance endocytosis of DNA into the nucleus. These complexes were formed between PAMAM dendrimers and DNA through electrostatic interactions of the negative phosphate groups of DNA and the positive dendrimer terminal amino groups, depicted in Fig. 1(c). Dendrimer-mediated transfection efficiency was found to depend on the dendrimer/DNA ratio as well as the dendrimer generation [36, 37]. The structural flexibility of the dendrimer due to the core-type/multiplicity was also found to play an important role in complexation and transfection [38]. Modifications to the dendrimer surface, such as attaching sugar molecules (cyclodextrins) [39] and hydrophobic dye molecules (Oregon green 488) [40], have been found to improve transfection efficiency; however, the underlying transfection mechanisms are still unclear. However, the molecular mechanisms underlying complexation between short doubled stranded RNA (siRNA) and PAMAM dendrimers have been described by Pavan et al. [41] using molecular simulation, NMR and electrophoresis assays. Electrostatic complexation of anionic DNA with cationic dendrimers has also been shown to result in the formation of DNA-linked PAMAM nanoclusters as described by MD simulations by Madal et al. [42]. Conti et al. [43] used similar siRNA-G4 PAMAM complexes to develop an oral inhalation formulation to silence genes in lung alveolar epithelial cells, towards the treatment of pulmonary disorders including lung cancer and cystic fibrosis.

2.3. Imaging agents

PAMAM dendrimers have also been conjectured as scaffolds for magnetic resonance imaging (MRI) contrast agents [44, 45], shown in Fig. 1(b), to improve contrast and decrease required dosage. Paramagnetic chelates are known to increase the relaxation rates of surrounding protons, and are widely used in MRI; however, they are rapidly cleared from vascular space. Large doses of these chelates are required to improve relaxation rates, which has resulted in concerns about metal ion toxicity. Conjugating these chelates to scaffolds, such as PAMAM dendrimers, reduces the dosage required for imaging, as well as improving their efficiency. The improved efficiency of these conjugates as imaging agents is due in part to changes in their pharmacokinetics. The retention of these conjugates in tissue is dependent upon the generation, charge and functionality of the dendrimers. Dendrimers with higher molecular weight were found to diffuse more slowly through the blood, which in turn increased their retention and effectiveness as imaging agents. Increasing dendrimer generation was also found to improve relaxivity because more chelates could be bound to dendrimers with larger numbers of terminal groups. Wiener et al. found that higher generation ammonia-core dendrimers (G6) conjugated to the chelate 2-(4-isothiocyanatobenzyl)-6-methyldiethylenetriaminepentaacetic acid were more efficient MRI contrast agents than those conjugated to G2 dendrimers [46]. In 1999 Bryant et al. continued this investigation for higher generation dendrimers. They found a limit in the improvement of the relaxivity for dendrimers of generation 7 and above. This relaxivity limit was thought to be due to the slow water exchange of bound water molecules with the bulk solvent [47]. Mekuria et al. have very recently demonstrated that trapped Gadolinium oxide nanoparticles in PEGylated G4.5 PAMAM dendrimers could be used as *dual* MRI contrast agents which showed greater signal responses than currently used clinical agents [48]. Dual contrast agents can be used to improve clinical diagnosis, since single modal signals can give false positive diagnosis of lesions due to background signals in neighbouring tissues. However, bioaccumulation of these dendrimer-conjugates in organs remains an issue, limiting their clinical applications [49].

2.4. Antimicrobials

PAMAM dendrimers have also been shown to exhibit antimicrobial properties, or improve the effectiveness of existing antimicrobials via conjugation, and their efficacy seems to depend on the dendrimer size/generation, surface chemistry and concentration, as well as the bacteria type due to the composition and structure variations of gram-negative and gram-positive bacteria [50].

Calabretta et al. [51] and Lopez et al. [52] demonstrated concentration-dependent antibacterial properties of amine terminated PAMAM dendrimers (G3 and G5). With positively charged amine groups, they preferentially bound to bacterial membranes which have a higher charge density than eukaryotic cells. PEGylation was thought to shield the terminal amino groups, resulting in decreased binding and thus decreased membrane interactions. However, it was found that PEGylation of PAMAM reduced toxicity to gram positive bacteria and human corneal epithelial cells (HCECs) but not to gram negative bacteria. It was also found that there was no difference in the antibacterial properties of the G3 and G5 dendrimers, despite the increase in charge density of G5. Wang et al. [26] studied the effect of surface chemistry of PAMAM dendrimers (with –OH, –COOH and -NH_2 terminal groups) on their antibacterial activity against *E. coli* and their toxicity to human cervical epithelial cells. All the dendrimers had high antibacterial activity against *E. coli*; however, NH_2-terminated dendrimers were also cytotoxic to the mammalian cells, where OH-terminated dendrimers were cytotoxic at concentrations of 1 mg/mL.

Despite the large number of studies, the application of dendrimers in biomedicine remains hindered due to a lack of understanding of the relationship between PAMAM dendrimer physicochemical properties and the mechanism of their cellular uptake and cytotoxicity. The variations in cell response found in cytotoxicity studies, due to different physicochemical properties of dendrimers, and the possible underpinning fundamental interactions are discussed below.

3. Cytotoxicity and uptake of PAMAM dendrimers

3.1. Cellular uptake mechanisms of PAMAM dendrimers: endocytosis vs. passive diffusion

The mechanisms of dendrimer cellular uptake have been shown to vary considerably with their generation, functionalisation and concentration, although the exact roles of these parameters – individually and collectively – remain unclear. Cellular uptake and intracellular transport is known to be dependent on the dendrimer surface charge and the cell type. The intracellular fate of dendrimers depends on the mechanisms of their cellular uptake, where the size of vesicles, the type of proteins involved and the cell type in which they are found can vary considerably.

Albertazzi et al. [53] studied the impact of dendrimer surface chemistry (cationic, neutral and hydrophobic/lipidated) and size (G2, 4 and 6) on the uptake mechanisms by cervical cancer (HeLa) cells. The membrane affinity of the dendrimers was found to depend upon their generation or the amount of positive charges on their periphery (G6 > G4 > G2) which could be decreased by acetylation or increased by lipidation. Increased membrane affinity was also linked to increased cytotoxicity. The uptake of G4 cationic dendrimers was also compared between different cell types (HeLa, hepatocarcinoma (HepG2), neuronal-like (PC-12), lung fibroblast (MRC5)). Similarities were observed between the uptake mechanisms of HeLa and MRC5 cells whereas HepG2 showed stronger, faster uptake and PC-12 showed high membrane affinity but the slowest uptake.

Perumal et al. [54] studied the uptake mechanisms of G4 *cationic* and *neutral* PAMAM dendrimers as well as G3.5 *anionic* dendrimers into lung epithelial cells (A549), known to possess negative charges. The cell uptake was highest for cationic dendrimers which plateaued after 1 h, likely due to strong electrostatic interactions. The cationic and

neutral dendrimers were found to be taken up by non-clathrin and non-caveolae mediated endocytosis, whereas anionic dendrimers were partially taken up by caveolae in the A549 cells. This observation was in contrast to a study by Kitchens et al. [55] who observed co-localisation of dendrimers with clathrin markers in Caco-2 cells. El-Sayed et al. [56] found that low-generation dendrimers crossed Caco-2 cell monolayers faster than high-generation dendrimers, and that the uptake amount varied linearly with the dendrimer concentration and incubation time, consistent with an endocytosis uptake mechanism.

Whilst endocytosis is reported to be the main cellular uptake mechanism of PAMAM dendrimers, passive diffusion may still play a part in this process. Recently, the in vitro uptake mechanisms of PAMAM dendrimers were investigated for non-cancerous human keratinocyte (HaCaT) cells by Maher and Byrne [57]. Endocytosis [6] was the primary mechanism for the uptake of G4 and G6 PAMAM dendrimers, identified by ROS production and dendrimer localisation in the mitochondria after their escape from endosomes, using MTT and Alamar Blue dye-based assays. This intracellular pathway was consistent with that reported by Mukherjee et al. [12]. After the HaCaT cells were treated with DL-buthionine-(*S,R*)-sulfoximine (BSO) to increase membrane permeability, the dendrimers were taken up passively. The dendrimers were found to act as antioxidants in the cytosol when taken up passively, rather than producing ROS. This shows that the cytotoxic response was influenced by the cellular uptake pathway, which in turn was influenced by dendrimer-membrane interactions.

Manunta et al. [58] found the removal of cholesterol from the plasma membrane resulted in a drastically decreased transfection efficient of genes delivered by cationic dendrimers. This showed that amine-terminated dendrimers interacted with cholesterol in the plasma membrane during endocytosis. This is one of several proposed endocytosis routes and highlights the importance of membrane composition on uptake dynamics.

3.2. Cytotoxicity of PAMAM dendrimers

PAMAM dendrimers have been shown to produce different cytotoxic responses from cells depending upon the dendrimer generation, concentration and surface chemistry. G4 are the most widely studied PAMAM dendrimers, with a diameter comparable to the thickness of a cellular membrane (~4.5 nm). These dendrimers have also been shown to encapsulate small guest molecules, making them suitable for a range of biomedical applications [59]. The responses of many cell types to PAMAM dendrimers have been evaluated using a variety of toxicity assays that investigate cell death, metabolism, enzyme leakage and DNA damage [11, 60–63]. Examples of recent cytotoxicity studies are summarized below in Table 2.

In 2010, Mukherjee et al. investigated the interaction between G4–6 PAMAM dendrimers and dermal (HaCaT) and colon (SW480) cell lines using cell viability assays including Alamar blue, MTT and Neutral red [11, 12]. It was found that toxicity varied between cell types as well as with dendrimer generation and concentration. PAMAM dendrimers were discovered to localise in mitochondria and produce reactive oxygen species (ROS) resulting in DNA damage and cell death. The cationic PAMAM dendrimers entered the cell through endocytosis and were transported in endosomes and localised in mitochondria. The dendrimers increased the internal pH of the mitochondria because of an acid-base equilibrium reaction between secondary amines and their conjugate base, resulting in the production of ROS. The differences in the toxic responses by different cell types when exposed to PAMAM dendrimers could be a result of different cell-membrane compositions or cell anti-oxidant levels that combat ROS production. DNA damage, measured using a TUNEL (Terminal deoxynucleotidyl transferase (TdT) dUTP Nick-End Labelling) assay, was shown to increase with dendrimer generation, possibly due to the corresponding increase in charge density which promotes dendrimer binding to negatively charged DNAs. Such strong interactions between DNA and PAMAM dendrimers [14] have also made them of interest for gene delivery applications [67] as discussed in Section 2.2.

Particle size and zeta potential measurements by Mukherjee et al. [11, 12] indicated significant adsorption of protein on PAMAM dendrimers in growth media, with the adsorbed amount increasing with the dendrimer generation. The formation of such a protein corona has been shown to significantly alter interactions between dendrimers and cellular membranes. For example, Halets et al. showed interactions between G4 dendrimers (with 25% of terminal groups modified with carbon chains) and blood proteins reduced their toxicity towards red blood cells [64]. Naha et al. found the zeta potential of cationic dendrimers changed from positive to negative in growth media, indicative of the formation of a protein corona. Similarly, Naha et al. also found generation-dependent toxicity for cationic PAMAM dendrimers towards mouse macrophage cells (J774A.1), and that the production of ROS in the toxicity pathway was followed by an inflammatory response [60].

The surface chemistry of dendrimers has been found to influence their cytotoxicity. Differences in toxicity have been observed for PAMAM dendrimers functionalised with hydrophobic [61, 64], PEG [51, 52], —OH [68] and pyrrolidine [66] terminal groups. In 2012, Albertazzi et al. investigated the effect of hydrophobic chain functionalisation on the cytotoxicity of G4 PAMAM dendrimers interacting with primary neuronal cultures and the central nervous system (CNS) of animals [61]. They found that nanomolar quantities of G4 PAMAM dendrimers with 25% of terminal groups modified with carbon chains (G4-C12) resulted in apoptosis (cell death), whereas the same quantity of G4 PAMAM, without additional functionality, is non-cytotoxic. It was also found that G4 PAMAM could diffuse through the brain parenchyma whereas G4-C12, due to its lipophilic nature, could not. These diffusion characteristics make PAMAM dendrimers of interest for neural drug delivery, where they could be used to help therapeutics pass the blood-brain barrier (BBB) [69].

Hong et al. used Luciferase (Luc) and Lactate dehydrogenase (LDH) enzyme leakage assays to evaluate damage to the cellular membranes of human epithelial carcinoma (KB) and rat fibroblast (Rat2) cell lines when exposed to G5 PAMAM dendrimers with and without acetamide functionalisation [65]. Enzyme leakage was shown to increase with G5 PAMAM dendrimer concentration for both cell lines; however, when the terminal groups of the dendrimers were functionalised with acetamide, no leakage was observed. The charge neutrality of acetamide terminated dendrimers reduced their toxicity and ability to transfect cells. This demonstrated the importance of dendrimer surface charge on interactions with cellular membranes. The functionalisation of the terminal amine groups with PEG was also found to reduce toxicity by Calabretta et al. [51] and Lopez et al. [52].

In summary, multiple studies have shown that a large number of factors affecting PAMAM cellular uptake and trafficking and conflicting conclusions exist regarding different pathways and the subsequent cytotoxic response [70]. It is thus important to understand the underpinning interactions between the dendrimers and cellular membranes. The complexity of the membranes, consisting of hundreds of different lipids with different headgroups and chain lengths alongside various proteins and carbohydrates, makes it difficult to study such interactions in vivo. Consequently, simplified membrane models have been developed so that the physical properties of the membrane such as elasticity, thickness and lipid ordering can be studied in the presence of dendrimers. These models are also used widely for the study of the cellular uptake of other nanoparticles such as gold, silver, silica and carbon nanotubes (e.g. see a recent review [6]).

4. Interactions between PAMAM dendrimers and model membranes

Since the development of the first Langmuir-Blodgett trough in the 1920's, model membranes have since been developed by several groups to explore interactions between lipid molecules and proteins, pharmaceuticals and nanoparticles [6, 71] by observing both structural and

Table 2
Recent cytotoxicity studies of PAMAM dendrimers.

Size	Dendrimer surface functionality	Cell Line	Assay types	Comment	Ref
G4–6	NH_2	Human keratinocyte (HaCaT) & Colon cancer (SW480)	Alamar Blue MTT Neutral Red & TUNEL	Toxicity increased with dendrimer generation; SW480 showed greater oxidative stress, apoptosis, & DNA damage in response to exposure.	[11, 12]
G3–6	NH_2 & 25% C_{12}	Red blood cells (RBC)	Hemolysis	Blood proteins and DNA complexed with dendrimers and reduced toxicity.	[64]
G4–6	NH_2	Mouse macrophage (J774A.1)	Alamar Blue, MTT, Intracellular ROS generation, MIP-2, IL-6, & TNF-α	Toxicity (ROS production & inflammatory response) increased with dendrimer generation.	[60]
G4	NH_2 & 25% C_{12}	Mouse primary neuronal cultures & Central nervous system (CNS) of live mice	Apoptosis staining Immunostaining & TUNEL	Penetration of NH_2-dendrimers into brain parenchyma but not 25% C_{12}-dendrimers; low toxicity of NH_2-dendrimers at nM concentrations; apoptosis due to 25% C_{12}-dendrimers	[61]
G5 & G7	NH_2, Acetamide & Folic Acid	Human cervical cancer (KB) & Rat fibroblast (Rat2)	Luc, LDH, & Temp dependent dye diffusion	G5 dendrimer-induced membrane permeability was reversible; acetamide functionalisation reduced toxicity; at 6 °C no enzyme leakage was observed for G5 NH_2 but is for G7 NH_2.	[65]
G5	NH_2 & 43% PEG	*P. aeruginosa* *S. aureus*	MTT	NH_2-dendrimers showed antimicrobial efficacy; PEG coating reduced toxicity to gram-positive bacteria.	[51]
G3 & G5	NH_2 & (6–84%) PEG	*P. aeruginosa, S. aureus* & human corneal epithelial cells (SV40-HCEC)	Minimum inhibitory concentration (MIC) & MTT	No change in toxicity was observed for different dendrimer generations; 6%-PEG coated dendrimers decreased toxicity to gram-positive bacteria and host HCEC cells but maintained high toxicity to gram-negative bacteria.	[52]
G4	NH_2 & Pyrrolidine	Chinese hamster fibroblasts (B14), embryonic mouse hippocampus (mHippoE-18) & rat liver (BRL-3A)	MTT, ROS generation, Mitochondrial membrane potential & Apoptosis	Pyrrolidine functionalisation reduced toxicity towards all three cell lines.	[66]
G3.5 & G4	NH_2 & OH	Chinese hamster ovary (CHO) & human ovarian carcinoma (SKOV3)	MTT, ROS generation, Antioxidant activity (ABTS), Mitochondrial membrane potential & AO/EB staining	μM quantities of cationic G4 reduced viability to below 50%; anionic G3.5 was much less toxic.	[62]
G4	NH_2	Human lung cells (WI-26 VA4)	Gene expression, RNA Expression (RT-PCR), Mitotracker, Mitochondrial membrane potential, MTT, Cytochrome C & TUNEL	Cell viability was decreased in a dose dependant manner; Damaged mitochondria resulted in apoptosis.	[63]
G5	NH_2 & Lauric, Myristic, Palmitic fatty acids	Mesenchymal stem cells	Cellular uptake (FACS), Gene delivery & Cell viability (Rezasurin reduction assay)	Improved gene delivery and decreased cytotoxicity was observed for dendrimers with fatty acid conjugation, with the highest efficiency observed for dendrimers with shortest hydrophobic chains.	[67]
G4 & G6	NH_2	Human keratinocyte (HaCaT) with BSO treatment	Alamar Blue, MTT & ROS generation	BSO showed increased membrane permeability and therefore increased passive uptake which depended on dendrimer generation. Passive uptake of dendrimers decreased oxidative stress, with the dendrimers acting as antioxidants.	[57]

energetic changes qualitatively and quantitatively. These models include lipid monolayers (first studied by Langmuir and Blodgett [72–74]), mesophases [75, 76], bilayers [76, 77], multilayers, vesicles/liposomes [78] and computational models [79] (Fig. 2). These models can mimic the structural organisation of cellular membranes as well as the charge by varying the lipid composition. Lipids can have a number of different charged headgroups (e.g. phosphatidylethanolanmine (PE), phoshatidic acid (PA), phosphatidylglycerol (PG), phosphatidylinositol (PI)), as well as have carbon-chains of different lengths and saturation degrees. This variation results in different charge densities, chain fluidities and liquid crystalline phases. Due to the wide variety of cellular membranes present within a cell (plasma membrane, organelles, and nucleus) and between different cell types, there is no 'one size fits all' model. However, by varying composition, combining several of these models, and using a range of characterisation techniques, it has been possible to gain physical insights into the fundamental interactions between dendrimers and lipid membranes. The use of these models allows both qualitative and quantitative comparisons of PAMAM dendrimer physicochemical properties on interactions with cell membranes of varying properties, which we briefly review below.

4.1. Interactions between PAMAM dendrimers with supported lipid bilayers (SLBs)

Supported lipid bilayers (SLBs) are well suited for studying the dendrimer-membrane interactions, as they lend themselves readily to quantitative analysis using a range of surface sensitive techniques such as X-ray and neutron reflectivity (XRR and NR) [14, 80, 81], atomic force microscopy (AFM) [82–84], ellipsometry [14, 85], quartz crystal microbalance with dissipation (QCM-D) [81, 85, 86], NMR [87], differential scanning calorimetry (DSC) and Raman spectroscopy [88].

Both symmetric and asymmetric bilayers can be formed via the vesicle rupture method [89] at a solid substrate (e.g. silica [81, 89] and mica [82, 90, 91]). In addition, SLBs can also be prepared via two sequential depositions of Langmuir monolayers onto a solid support [83]. The presence of the solid support could affect the bilayer structure and

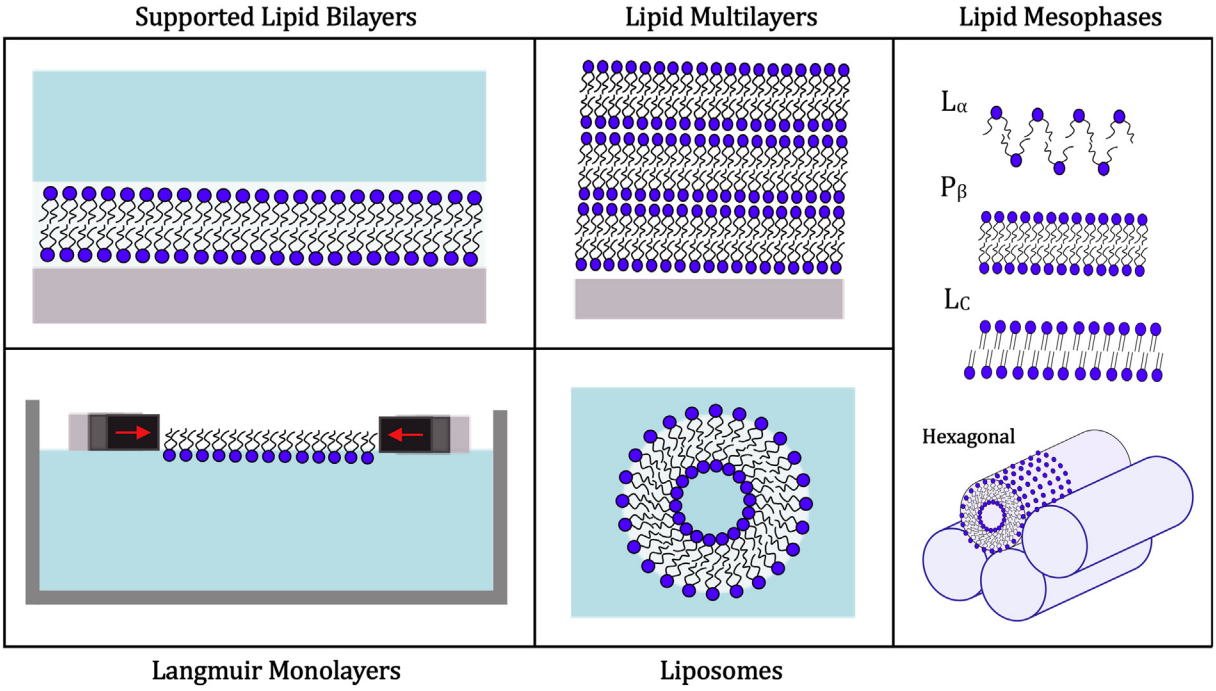

Fig. 2. Model membrane systems used for nanoparticle-membrane interaction studies: one lipid leaflet (monolayers), two leaflets (bilayer) or several stacked bilayers (multilayers). Liposomes (made up of an enclosed lipid bilayer) and the liquid crystalline phases of lipids (including fluid (L_α), ripple (P_β) and crystalline (L_c) lamellar phases and hexagonal phase) can also be used to study the deformation energetics during endocytosis and membrane fusion.

fluidity, e.g. via the lipid-substrate electrostatic interactions and mismatch between the membrane natural curvature and the flat substrate, thus affecting lateral molecular diffusion, lipid domain formation and the reactivity of the SLB.

Cell membranes modulate their lipid phase behaviour by varying their composition. This results in different crystalline lipid phases, important for membrane fusion [92–94] and the formation of lipid rafts (microdomains of one lipid type) [95], conjectured to regulate membrane signalling and cellular entry [87]. The molecular packing and thus the bilayer structure can be tuned by using different lipids to mimic different membranes [83]. An understanding of how the composition and phase behaviour of lipid membranes influence interactions with dendrimers is therefore important in understanding their effects on cellular processes. This could be readily accessed by using SLBs. Large areas of defect-free DOPC and DPPC lipid bilayers have been successfully created using the vesicle-fusion method, with and without the addition of calcium ions [83]. DOPC and DPPC have different transition temperatures (−16.5 °C and 41.3 °C, respectively), which means they are in different phase states at room temperature which can affect bilayer formation. Table 3 lists several studies of interactions between SLBs of different compositions and PAMAM dendrimers of different generations and surface functionalities.

Parimi et al. [97] used optical waveguide light mode spectroscopy (OWLS) and AFM to study mass and morphological changes of DMPC (1,2-dimyristoyl-sn-glycero-3-phosphocholine) SLBs in the presence of NH_2 terminated G2, G4 and G6 PAMAM dendrimers as shown in Fig. 3(a–c). It was found that an increase in the dendrimer concentration caused the existing defects to expand and encouraged formation of new holes in the bilayers. Lipids removed from the bilayer in the hole formation wrapped around the G6 dendrimers, forming aggregates (dendrisomes) in solution, some of which adsorbed to the exposed substrate, also observed by Mecke et al. [84, 96]. As described by several other AFM studies [65, 84, 96, 99], higher generation (G4 and G6) dendrimers caused lipid desorption to a larger extent, compared to lower generation (G2) dendrimers, due to their increased size and charge density. Hong et al. [65] and Mecke et al. [84, 96] used similar systems to study the effect of dendrimer surface functional groups on their interactions with DMPC SLBs. They found that low generation acetylated dendrimers did not initiate pore formation, which was consistent with in vitro results discussed in Section 3. The smaller defects were found to decrease in size over time, but larger defects fused together so that they were no longer isolated. Lower generation (G3) of acetamide- and amine-terminated PAMAM dendrimers absorbed to bilayer edges rather than removing lipids. Hong et al. [65] cooled DMPC SLBs to create coexisting regions of a gel and a fluid phase. The gel phase was unaffected by the presence of dendrimers, whereas the fluid phase was disrupted. The gel phase has a higher elastic modulus than the fluid phase and thus would require more energy to deform in the presence of dendrimers. This result highlights the importance of crystalline structure on PAMAM-membrane interactions, as also reported by Mecke et al. [84, 96].

Using differential scanning calorimetry (DSC) and Raman spectroscopy, Gardikis et al. [88] showed that DPPC SLBs underwent a phase transition from gel to a liquid-crystalline after a pre-transition stage. The addition of positively charged amine-terminated G4 and negatively charged carboxyl-terminated G3.5 PAMAM dendrimers at different concentrations altered these transitions, attributed to re-organisation of the lipids in the bilayer. Increased acyl chain fluidity as inferred from the Raman peak shifts indicated the incorporation of the dendrimers into the bilayer. Despite being of similar size (~4 nm) and having the same number of terminal groups, more of the G4 dendrimers were found to incorporate into the bilayers than the G3.5 dendrimers, which points to the influence of the dendrimer surface charge on their interactions with the zwitterionic lipid DPPC.

Most biological membranes have a net negative charge; therefore, it is important to understand the influence of bilayer composition and charge on PAMAM-membrane interactions. Åkesson et al. [81] used QCM-D and neutron reflectivity (NR) to study interactions between G6 PAMAM and POPC and mixed POPC/POPG SLBs. NR showed very low adsorption of G6 PAMAM on the POPC SLBs; however, it suggested major structural changes in the mixed POPC/POPG bilayers attributed to the attractive interaction between oppositely charged G6 and POPG, with the data fitted to a structure comprising alternating layers of bilayers and dendrimers. The lipid headgroups and dendrimers could not be

Table 3
Studies of PAMAM dendrimer interactions with SLBs.

Size	Dendrimer surface functionality	Lipid	Technique	Comment	Ref
G5 & G7	NH_2, acetamide & folic acid	DMPC	AFM	NH_2 dendrimers caused generation-dependent hole formation, and acetylated dendrimers did not cause hole formation. Gel phase was unaffected by dendrimers.	[65]
G3-G7	NH_2, carboxyl & acetamide	DMPC	AFM	Density of holes in membranes increased with dendrimer concentration and generation. Aggregation of high generation dendrimers and lipids in solution formed 'dendrisomes'.	[84, 96]
G2, G4 & G6	NH_2	DMPC	QWLS & AFM	Higher generation dendrimers caused more pronounced lipid desorption.	[97]
G3.5 & G4	NH_2 & carboxyl	DPPC	DSC & Raman spectroscopy	More G4 dendrimers were found incorporated into bilayers than G3.5.	[88]
G6	NH_2	POPC, POPC/POPG	QCM-D & NR	Structural changes were observed in mixed bilayers due to attractions between dendrimers and anionic POPG, and data fitting indicated partial intercalation of the dendrimers in the membrane.	[81]
G4	NH_2	PS/PC	QCM-D, NR & ellipsometry	G4 absorbed to all membrane compositions in a concentration-dependent manner and translocated through membranes. Increased salt concentration decreased dendrimer absorption.	[85]
G2, G4 & G6	NH_2	POPC	NR & ellipsometry	Translocation of low generation dendrimers through SLB and partial destruction of membrane caused by G6	[14]
G5 & G7	NH_2	DMPC	Solid state NMR	Dendrimers decreased the flexibility of acyl chains due to their partial insertion into membranes.	[87]
G4.5 & G5	NH_2 & COONa	DPPC-d62/DPPG	SFGS	Lipid displacement was observed. Cationic G5 caused more disruption than anionic G4.5. Dendrimers preferentially interacted with the gel phase.	[98]

distinguished using the model, due to either partial intercalation of the dendrimers or fluctuations in curvature. Yanez Arteta et al. [85] used the same techniques (QCM-D and NR) alongside ellipsometry to study the absorption of G4 PAMAM on mixed PS-PC SLBs with different charge densities due to varying PS/PC composition. G4 dendrimers were found to adsorb to all the membrane compositions, but the adsorbed amount depended on the dendrimer concentration, and decreased with the increasing salt concentration or pH due to the screening effect. G4 dendrimers were also found to translocate through the membranes subsequent to adsorption. This result was consistent with the findings of Ainalem et al. [14], who showed translocation of low generation (G2 and G4) PAMAM dendrimers through POPC SLBs using ellipsometry and NR. Ainalem et al. also found that G6 dendrimers penetrated into the bilayer, causing partial bilayer destruction. These results indicate that PAMAM dendrimers can bypass cellular membranes by direct penetration, contrary to many of the results from toxicity assays.

Insertion of dendrimers into the bilayer could cause structural disorder, affecting membrane fluidity. Using solid state NMR, Smith et al. [87]

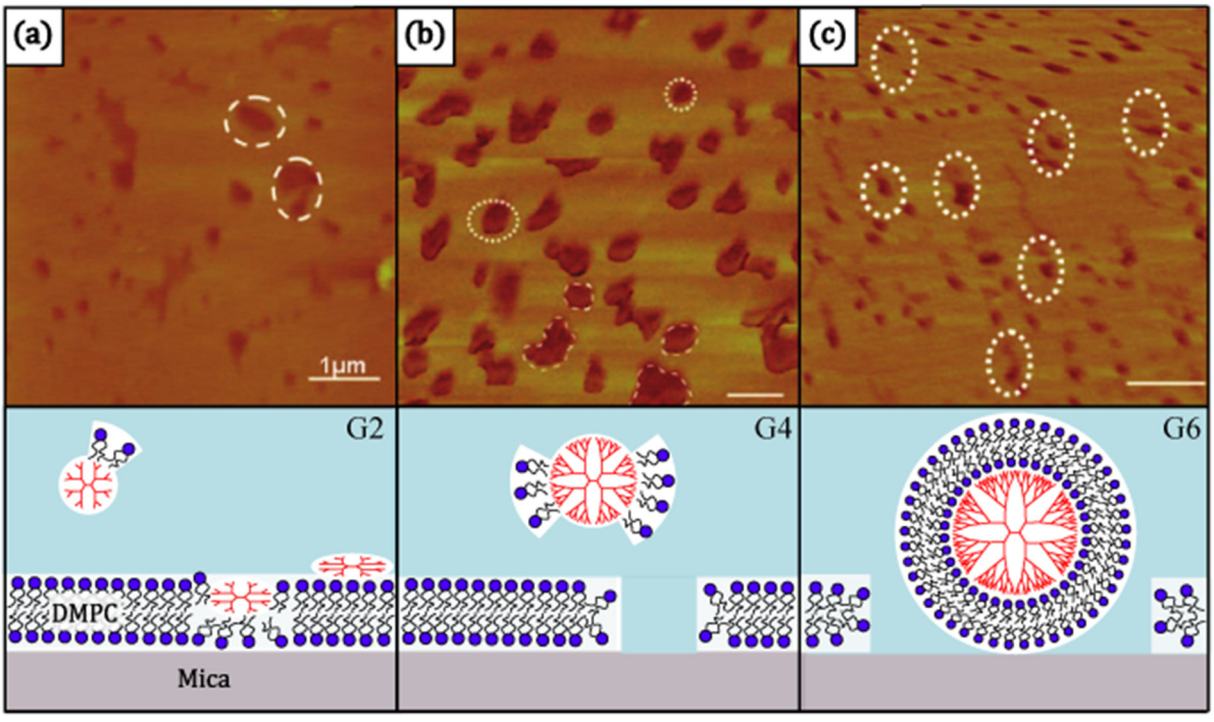

Fig. 3. AFM images of a DMPC SLB 20 min after incubation with (a) G2 (b) G4 and (c) G6 PAMAM dendrimers. Hole formation and growth was found to be generation dependant, with the extent of bilayer removal following the order G6 > G4 > G2. G4 and G6 dendrimers were found to expand existing defects (dotted lines), this was thought to lead to the formation of dendrimer-lipid aggregates that were removed from the substrate into solution. For G6 dendrimers these aggregates were thought to consist of a lipid bilayer wrapped around a dendrimer, or a 'dendrisome'. AFM images adapted with permission from [97]. Copyright 2008 American Chemical Society.

found that G5 and G7 dendrimers decreased the flexibility of acyl chains of DMPC SLBs. Partial insertion of PAMAM dendrimers was thought to result in the formation of a void region in the membrane, increasing the motions of acyl chains, and the bilayer would also become thinner as a result. This effect was also described by Mecke et al. [99] studying the interactions between the MSI-78 polymer, an analogue of an antimicrobial found in frog's skin, and a DMPC SLB using AFM and NMR.

Interactions between PAMAM dendrimers and asymmetric bilayers have also been studied. Keszthelyi et al. [98] created asymmetrical SLBs using Langmuir-Blodgett and Langmuir-Schafer deposition. Sum frequency generation spectroscopy (SFGS) was used to monitor interactions between NH_2- and COONa- terminated PAMAM dendrimers with a chain-perdeuterated zwitterionic (DPPC-d62) and anionic (DPPG) membrane outer leaflet. Reduction in —OH and —CH band intensities indicated a displacement of lipids and a change in the ordering of water molecules in the hydration layer at the bilayer interface. Positively charged G5-NH_2 was found to cause more disruption than negatively charged G4.5-COONa to both the DPPC and DPPG outer leaflet evident from a larger reduction in the —OH band, as well as increasing the ordering of alkyl chains compared to G4.5-COONa. The expansion of existing defects by positively charged dendrimers was also found by Hong et al. using AFM as discussed previously [65], who also found that the dendrimers preferentially interacted with the fluid phase and not with the gel phase; whereas Keszthelyi et al. showed the opposite, i.e. dendrimers preferentially interacted with the gel phase.

In summary, interactions between PAMAM dendrimers and SLBs have been studied using various techniques including AFM, NR, QCM-D, DSC and Raman spectroscopy. Most of these studies have found that higher generation dendrimers cause more disruption to SLBs than lower generations. AFM has been used to visualise the pore formation in SLBs caused by the removal of mass by dendrimers. Mass removal from the SLBs was found to increase with dendrimer concentration and generation and resulted in the formation of dendrimer-lipid aggregates. The size of these dendrimer-lipid aggregates has been measured using DLS and it was found that lipid bilayers wrap around higher generation dendrimers (>G5) forming 'dendrisomes'. Using NR, dendrimers have been found to translocate through SLBs, which indicates the possibility of passive transfer through cell membranes as suggested by in vitro studies discussed in Section 3 [57]. The energetics of these interactions has been explored using DSC and Raman spectroscopy, revealing changes in the fluidity of lipid acyl chains in the presence of dendrimers dependent upon dendrimer generation and charge. The effect of lipid and dendrimer charge on SLB-dendrimer interactions has also been explored using sum frequency spectroscopy and varying the composition of SLBs and terminal groups of dendrimers. It was found that positively charged dendrimers caused more disruption to neutral or positively charged membranes than negatively charged dendrimers. Disruption of bilayers by dendrimers was shown to be dependent on the fluidity of the lipid membrane, with fluid phase regions being more disrupted by dendrimers than gel phase regions. Membrane fluidity is linked to membrane composition which can vary within different organelles within a cell (mitochondria, nucleus etc.), cell type (for example cancer cells have more fluid membranes compared to non-tumor cells) or during cell processes such as morphogenesis when some types of specialized cells form different types of tissues. Therefore, it is important to understand how fluidity and composition effect interactions with dendrimers for biomedical applications.

4.2. Interactions between PAMAM Dendrimers and Langmuir monolayers

Langmuir monolayers are made up of one leaflet of a lipid at the liquid-air interface, typically formed by spreading lipids dissolved in a volatile organic solvent onto an aqueous subphase within a Langmuir-Blodgett trough. As the monolayer is compressed, a surface pressure (π) versus surface area (A) isotherm is recorded and the phase (or aggregation state) of the lipids at different surface pressures can be determined. The derivative of this curve can be used to find the monolayer elasticity or fluidity [100]. The composition of the monolayer can be tuned, and the packing of the monolayer can be adjusted by varying the surface pressure, allowing the effect of different nanoparticles on the monolayers of different designated properties to be studied. These monolayers can be observed using fluorescence microscopy or Brewster angle microscopy (BAM), and additionally the monolayers can be transferred to a substrate, such as mica, at a designated surface pressure to create supported monolayers or SLBs. There have only been a small number of studies on interactions between PAMAM dendrimers and Langmuir-monolayer models. However, monolayers have been widely used to explore interactions with other nanoparticles, including gold [101] and silica [102] as well as pharmaceuticals [103].

Cancino et al. [104] investigated the interactions between PC monolayers and G2 PAMAM dendrimers, single walled carbon nanotubes (SWCNT) and dendrimer-SWCNT conjugates (G2, G4, G6). The surface pressure of the monolayer was recorded as a function of molecular area (π-A) alongside BAM observations and dilatational surface elasticity measurements. The addition of G4-SWCNT and G6-SWCNT to the monolayers produced similar π-A isotherms to the control DPPC monolayers apart from a change in collapse pressure, which indicated little to no change to the lipid packing but adsorption of the complexes at the interface. However, compared to the pure lipid monolayers, a higher compressibility modulus of monolayers was observed with the addition of G2 PAMAM, as well as a shift in the maximum packing (or collapse pressure) with the addition of G2 PAMAM, SWCNTs and G2-SWCNT conjugates. These results suggested their incorporation into the monolayer, causing the lipid molecules to be less densely packed. Dilatational surface elasticity measurements showed a decrease in the surface elasticity of all the monolayers due to the incorporation of the dendrimer complexes. BAM images revealed the formation of new morphologies in the presence of SWCNTs but not G2-SWCNT complexes. The differences in interactions between the SWCNT and dendrimer-SWCNT complexes, and the DPPC monolayer remain to be fully understood.

Tiriveedhi et al. [105] studied the effect of G1 and G4 PAMAM dendrimers on the surface pressure of lipid monolayers (PC and PC/PG (3:1)). Addition of the dendrimers to the subphase caused an increase in the monolayer surface pressure Δπ when the initial pressure π_0 it is <30 mN/m (cf. Fig. 4b) which is comparable to pressure experienced in a biological membrane. This suggested the penetration of the dendrimers into the monolayer, up to a threshold surface pressure or a threshold lipid packing density, above which dense lipid packing did not allow dendrimer incoporation. The threshold surface pressure was the same for all the monolayer compositions and dendrimer generations studied. The increase in surface pressure was found to be greater for the monolayers containing negatively charged PG lipids, indicating more dendrimers penetrating monolayers containing oppositely charged lipids. Such lipid layer penetration by dendrimers has also been reported for SLB systems as discussed in the previous section. A threshold surface pressure for nanoparticle insertion has also been observed for other nanomaterials such as gold [101].

More recently, Wilde et al. [106] studied the effect of the concentration of carboxylate- (G4.5) and amine- (G5) terminated dendrimers on their incorporation into anionic DPPG monolayers. Both dendrimers were found to insert themselves into the monolayer at surface pressure of 21 mN/m, but exhibited differences in surface pressure relaxation, as the anionic G4.5 dendrimers took longer to equilibrate within the monolayer. There was little or no dendrimer penetration into DPPC monolayers at low dendrimer concentration, but it became more pronounced at higher dendrimer concentrations. The addition of sodium chloride was found to decrease the amount of G4.5 dendrimers penetrating DPPG bilayers, possibly due to charge screening. Fourier-transform infrared spectroscopy (FTIR) confirmed the presence of PAMAM dendrimers at the lipid-water interface and the adsorption varied considerably with membrane composition. These findings were

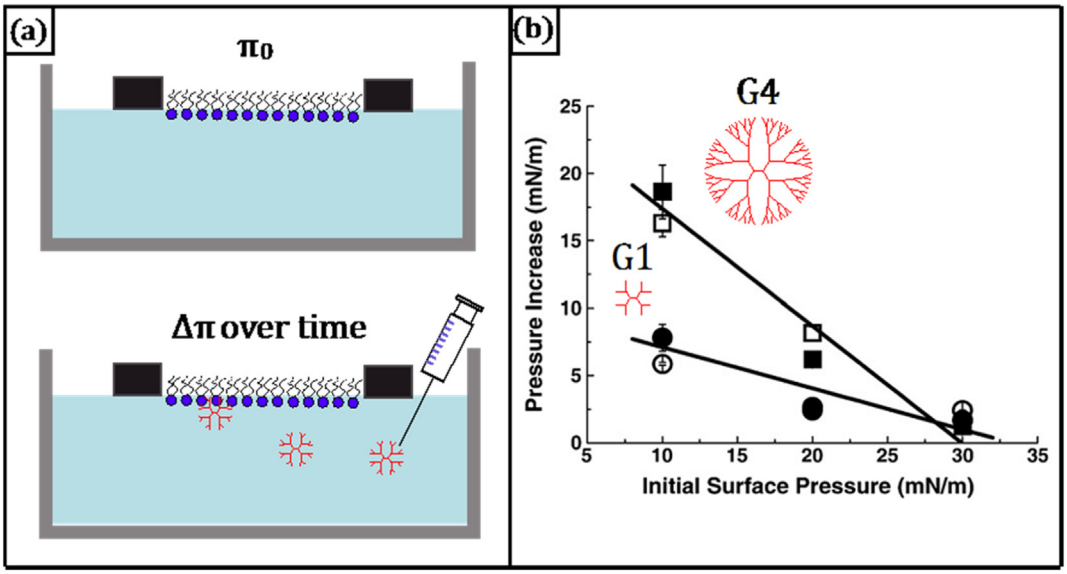

Fig. 4. (a) The change of surface pressure (π) over time of Langmuir monolayers can be monitored with the addition of dendrimers to the subphase. (b) Incorporation of PAMAM dendrimers into a Langmuir monolayer was shown to depend upon the the initial surface pressure before injection of dendrimers into the subphase. The maximum/threshold surface pressure of 30mN/m was shown to be the same for G1 and G4 dendrimers; however, G4 PAMAM showed a greater increase in the surface pressure than G2 at lower initial surface pressure. Isotherm adapted from [105] copyright 2011, with permission from Elsevier.

consistent with other studies reporting differences in membrane interactions with anionic or cationic dendrimers [107]. Interactions between PEG 20,000 and the monolayers were used for comparison with the charged dendrimers, and no insertion of PEG into either PG or PC membranes was observed. PEG has been used previously to decrease the toxicity of cationic PAMAM [51, 52] due to decreased insertion into the membrane and the screening of charges, causing less disruption to the cell membrane.

Despite the small number of studies undertaken, surface pressure isotherms of monolayer models have been able to probe interactions that lead to the insertion of cationic and anionic dendrimers of varying generation or size. The insertion dynamics has been shown to depend on the dendrimer charge, size and membrane composition. Lipid monolayer models can also be investigated with AFM once transferred to a substrate or used to create SLBs and probed with other techniques such as NR, as was discussed in section 4.1.

4.3. Interactions between PAMAM dendrimers and liposomes

4.3.1. Liposomes as model membranes

Liposomes (or vesicles) comprise single or multiple lipid bilayers that form a capsule enclosing an aqueous compartment, and can be made using several methods, including lipid thin film hydration (the Bangham method) [108], reverse phase evaporation, electrophoresis and using microfluidics [109]. The method used can influence the size and lamellarity of the liposome, whilst the lipid composition can also influence the liposomes size but also its stability, fluidity and charge. Liposomes are usually divided into sub-groups depending upon their lamellarity and size as shown in Fig. 5a. Multi-lamellar vesicles (MLV) are usually polydisperse and consist of several liposomes trapped inside each other, forming an onion-like structure. Uni-lamellar vesicles are then characterised by their size: small (SUV) 20–100 nm, large (LUV) >100 nm and giant (GUV) ~1000 nm. In addition to being used as cell membrane models, liposomes have been widely investigated as delivery vectors in drug delivery [109] due to their ability to encapsulate both hydrophilic and hydrophobic molecules, their biocompatibility and the possibility of chemical modifications for additional functionality.

Liposomes can be loaded with a self-quenching dye, such as Calcein, in the aqueous core to observe membrane disruption by dendrimers via dye-leakage assays, and the results complement those by cell leakage assays such as LDH, as described in Section 3. The change in the size and structure of liposomes in the presence of dendrimers can be monitored by dynamic light scattering (DLS), fluorescent microscopy (example Fig. 5c), small- and wide- angle x-ray scattering (SAXS/WAXS) (example Fig. 5b). Differential scanning calorimetry (DSC) can also reveal changes in the thermodynamic properties of liposomes, as demonstrated in Fig. 5d, such as the liquid-crystalline phase transition temperature and enthalpy.

4.3.2. Complexity of liposome-dendrimer interactions: effect of charge, membrane composition, and dendrimer size and concentration

Zhang and Smith [112] studied the interactions of positively charged G4–7 PAMAM and poly(lysine) dendrimers with anionic vesicles (3:7 POPE/POPA), using fluorescence assays to observe mixing of lipids and encapsulated content between vesicles, and leakage of the content. Lipid mixing was found to increase with increasing dendrimer generation, and with dendrimer concentration until a maximum before decreasing at higher dendrimer concentration. This concentration dependence was thought to be related to a maximum surface coverage of dendrimers on the vesicles that prevented their close approach. G7 PAMAM–DNA conjugates, with varying DNA phosphate group to dendrimer amine group ratios, induced different amounts of leakage from the anionic vesicles, with the maximum leakage/disruption observed at a 3:1 amine to phosphate ratio. These complexes at this ratio also induced high levels of cell transfection. This was thought to be related to changes in the charge-charge interactions between the conjugates and liposomes and depend highly on the membrane composition. In addition, the G7 dendrimers were also found to disrupt PEGylated vesicles by overcoming the hydration barrier and forcing apposed membranes to mix. Furthermore, ^{31}P NMR measurements showed that the G7 dendrimers induced the inverse hexagonal phase in the vesicle membranes, conjectured due to electrostatic interactions inducing inverse curvature in regions of the membrane, leading to packing stresses and enhanced lipid mixing.

Alongside the Langmuir monolayers model discussed in Section 4.2, Tiriveedhi et al. [105] also studied the changes in fluorescence

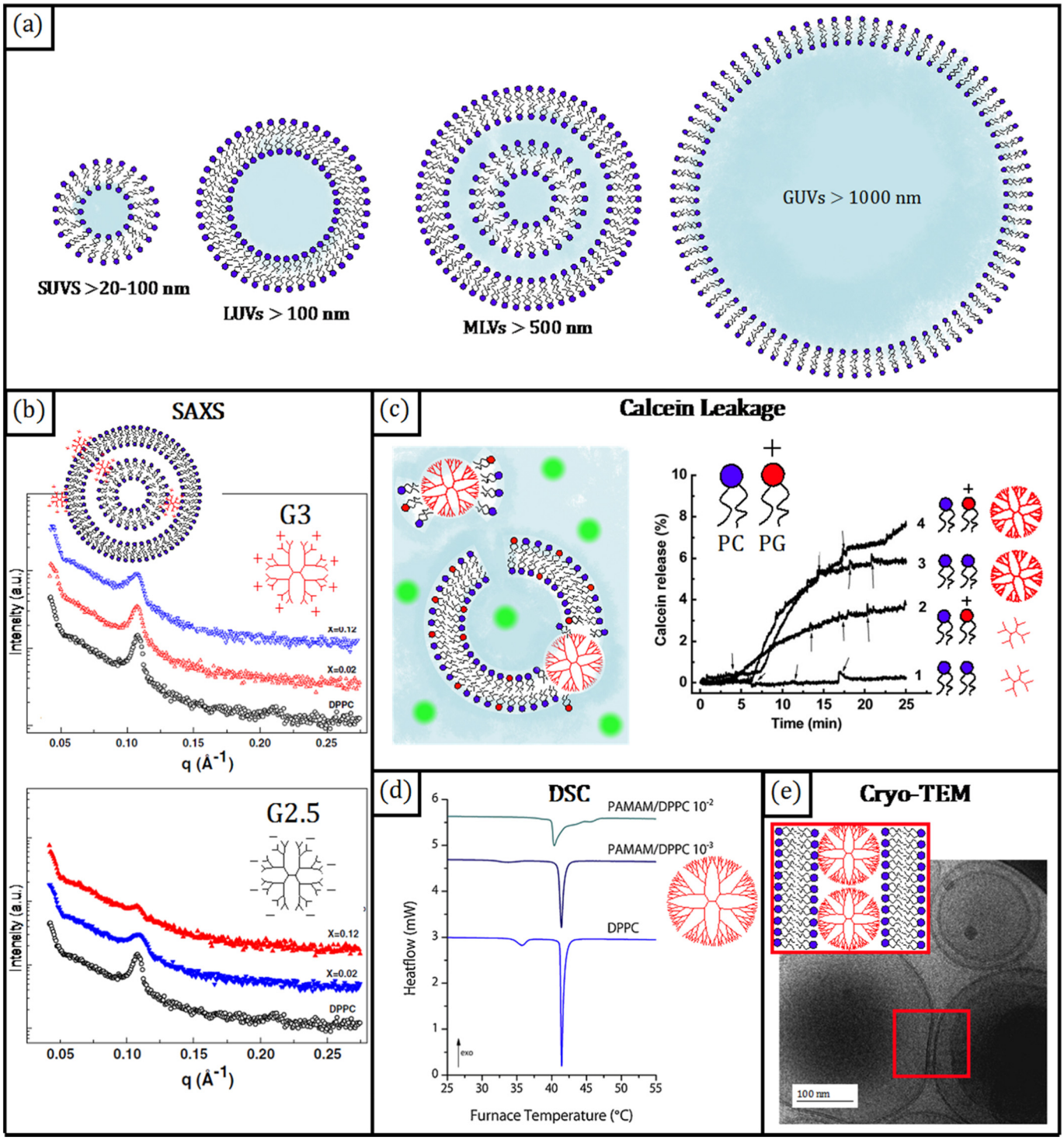

Fig. 5. (a) Liposomes are capsules made of lipid bilayers and can be catergorised by size, ranging from small (SUV) to giant (GUV) vesicles, and by their lamellar structure, i.e. unilamellar or multilamellar (MLV). Multiple techniques can be used to study the liposome properties. (b) Small angle X-ray scattering (SAXS) can monitor the change in position and width of Bragg peaks, related to the change in structure of MLVs. For instance, increasing dendrimer-to-lipid ratio (X) caused broadening of Bragg peaks associated with distruption to bilayer ordering, with negatively charged (G2.5) dendrimers found to cause more disruption than positively charged (G3) dendrimers. (c) Fluorometry, used in calcein release assays, showed higher generation dendrimers (G4) caused greater leakage of calcein from SUVs than lower generation dendrimers (G1), and greater leakage occurred from liposomes containing 25% cationic PG. (d) Differential scanning calorimetry (DSC) showed a concentration dependant change in the phase transtion and pre-transition peaks of liposomes in the presence of G5 dendrimers, indicative of changes in lipid packing and energetics. (e) Cryogenic- transmission electron microscopy (cryo-TEM) can image liposomes and provide information about their size and morphology, e.g. here in the presence of G6 dendrimers, where liposomes were found to aggregate and were bridged by the dendrimers. (b) Adapted from [107] copyright 2016, with permission from Elsevier, (c) Adapted from [105] copyright 2011, with permission from Elsevier, (d) Adapted from [110] copyright 2014, with permission from Elsevier, (e) Adapted from [111] copyright 2010 with permission from the PCCP Owner Societies.

anisotropy of FITC labelled G1 and G4 PAMAM dendrimers upon binding to SUVs of zwitterionic and anionic lipids (PC/PG) as demonstrated in Fig. 5c. It was found that the dendrimers preferentially bound to membranes containing negatively charged lipids and released larger amounts of encapsulated Calcein from those liposomes. It was also found that G4 caused more pronounced leakage from the liposomes

than G1, likely due to its larger charge density causing greater disruption to the vesicle membrane.

A recent study by Lombardo et al. [107] used zeta potential measurements to find the effective charge of DPPC MLVs in the presence of cationic G3 and anionic G2.5 PAMAM dendrimers. The zeta potential of the liposomes was found to vary linearly for both dendrimer generations, up to a threshold concentration where liposomes became saturated with dendrimers. Effective charge calculations suggested that approximately half of the dendrimer's surface charge contributed to the zeta potential, and this was rationalised by assuming dendrimers partially embedded in the bilayer. Bragg peaks from SAXS measurements, shown in Fig. 5b, revealed that there was no change in *d*-spacing (or bilayer thickness) of the MLVs upon dendrimer addition. However, broadening of the peaks with increasing dendrimer concentration indicated a loss in the number of bilayers, and this effect was also observed by Berenyi et al. with G5 dendrimers interacting with DPPC MLVs [110]. The bilayers in onion-like MLVs experience van der Waals, hydration and thermal undulation forces. The addition of dendrimers resulted in the repulsion of charged bilayers leading to decreased correlation, and eventually the formation of uni-lamellar vesicles. The negatively charged, G2.5 dendrimers were found to cause more perturbation than positively charged, G3 dendrimers. Adding the dendrimers at different stages in the production of liposomes was found to impact the dendrimer-liposome interactions. When dendrimers were added to extruded liposomes, aggregation occurred as demonstrated by Akesson et al. [111].

Kelly et al. [113] used a combination of isothermal titration calorimetry (ITC), DLS, AFM, TEM and molecular dynamics (MD) simulations to explore the interactions between G3–9 PAMAM dendrimers of different surface chemistry and liposomes made with zwitterionic and anionic lipids (DMPC and DMPG, respectively). Changes in enthalpy were observed only when dendrimers were titrated into liposomes made from anionic lipids. The heat release per dendrimer increased as these liposomes aggregated, and this continued up to a plateau at which point there were no more free lipids available to bind to the dendrimers. The binding stoichiometry of the dendrimers on liposomes was found to be generation dependent. For instance, larger dendrimers (>G6) could be completely wrapped in a lipid bilayer (*c.f.* Fig. 7b), whereas smaller dendrimers could not. Fig. 7c shows the enthalpy change and the binding stoichiometry (i.e. the number of lipids per dendrimer) for increasing dendrimer generation (or number of terminal amine groups). This was compared with MD simulations, which showed that low generation (<G4) dendrimers deformed and flattened on the bilayers (*c.f.* Fig. 7a), as proposed previously by Klajnert and Epand [114].

4.3.3. Lipid-dendrimer interactions: adsorption, intercalation, bridging, complexation, and 'Dendrisomes'

In a solid-state NMR study, Smith et al. [87] found cationic G5 and G7 PAMAM localised in the hydrophobic region of zwitterionic DMPC MLVs, which led to increased acyl chain ordering and decreased chain flexibility. The lipid tails intercalated into the G5 dendrimers, but the more closely packed surface groups of the G7 dendrimers suppressed the lipid penetration.

Åkesson et al. [111] found that adsorption of G6 PAMAM dendrimers to the surface of cationic liposomes (POPC/POPG) caused bridging attraction and aggregation between the liposomes, demonstrated in Fig. 5e. Cryo-TEM revealed that the dendrimers did not penetrate into the liposome inner water core, and that the distance between the aggregated liposomes corresponded to the dendrimer diameter, indicating that the liposomes were bridged by a single layer of dendrimers. The liposomes became destabilized at high dendrimer concentrations, likely due to the change in curvature introduced by the dendrimers making the vesicle architecture unfavourable, an effect modelled by Kelly et al. [113] and discussed above.

Using Calcein leakage assays, Karoonuthaisiri et al. [115] found that vesicle disruption was caused by vesicle aggregation, which was dependent upon membrane composition. The presence of DOPE, a lipid that prefers negative membrane curvature, in the membrane increased the extent of disruption by the dendrimers. It was suggested that membranes containing such lipids can wrap around large dendrimers to form 'dendrisomes'. The bending modulus was decreased in the membranes containing these lipids, which would allow the vesicles to deform more easily. Larger vesicles were more disrupted than smaller vesicles, attributed to distortions caused by vesicle aggregation. Unusually, the largest disruption was found at an intermediate dendrimer concentration, possibly due to the formation of a steric barrier by the adsorbed dendrimers to prevent vesicle aggregation at high surface coverage of the dendrimers, consistent with the observation reported by Zhang and Smith [112].

4.3.4. Thermodynamic insights: effect of dendrimers on membrane fluidity and phase transition

A DSC study by Klajnert and Epand [114] showed that G3 PAMAM dendrimers with three differing terminations, amine (NH_2), hexylamide (CH_3) and 50% N-(2-hydroxydodecyl) (or 50% C_{12}), affected the phase transitions and particularly the pre-transitional enthalpy in DPPC MLVs and DMPC SLVs. The pre-transitional enthalpy was lowered with the addition of dendrimers, indicating the transition between the rippled and lamellar gel phase was modified, this was likely due to the insertion of dendrimers into the bilayers effecting the cooperativity. How the dendrimers were added also influenced the thermotropic behaviour of the liposomes. For example, mixing dendrimers and lipids before hydration in the Bangham method (Method A; Fig. 6a) resulted in a symmetrical DSC transition peak, which indicated a uniform distribution of the dendrimers in the membranes. On the other hand, addition of the dendrimers during the hydration of the pre-formed lipid film (Method B; Fig. 6b) and addition to pre-formed vesicles (Method C; Fig. 6c) resulted in less penetration of the dendrimer into the multilayer vesicles, as indicated by asymmetrical transition peaks. C_{12} hydrophobic tails on 50% of the dendrimer periphery groups resulted in a more rigid, spherical particle, which caused more disruption to the liposomal membranes, shown in Fig. 6d. Hexylamide terminated dendrimers were thought to cluster at high concentration resulting in fewer interactions with the membrane, therefore the disruption did not increase with concentration for this functionalisation as is depicted in Fig. 6e. At low concentration these flattened dendrimers may incorporate in the hydrophobic portion of the bilayer, without causing much disruption.

Berenyi et al. [110] found that G5 PAMAM altered the pre-transition DSC peak of DPPC MLVs, shown in Fig. 5d, which indicated an interaction between dendrimers and the lipid polar headgroups and an increase in membrane fluidity, also confirmed by infrared spectroscopy. This demonstrated that the dendrimers effected the hydration level of the lipid interface and introduced a conformational disorder in the alkyl chain region. SAXS showed Bragg peaks due to the lipid bilayer were broadened when the MLVs were doped with 10^{-2} ratio of dendrimers to lipids, indicating a reduction in the number of bilayers in the MLVs, consistent with DSC measurements. A complex Bragg peak was observed in the SAXS pattern at 25 °C, corresponding to a highly swollen lamellar phase. The increased layer spacing was attributed to dendrimers embedding in the water shells between bilayers or increased electrostatic repulsion between the layers caused by embedded dendrimers. At 46 °C a larger bilayer spacing suggested shape change of dendrimers when interacting with gel/liquid crystalline phases, as observed in MD simulations from Kelly et al. [116] and discussed further in Section 4.4.

In summary, liposomes have been used as model membranes in a number of studies to investigate their interactions with PAMAM dendrimers. By using a range of techniques from SAXS to DLS the

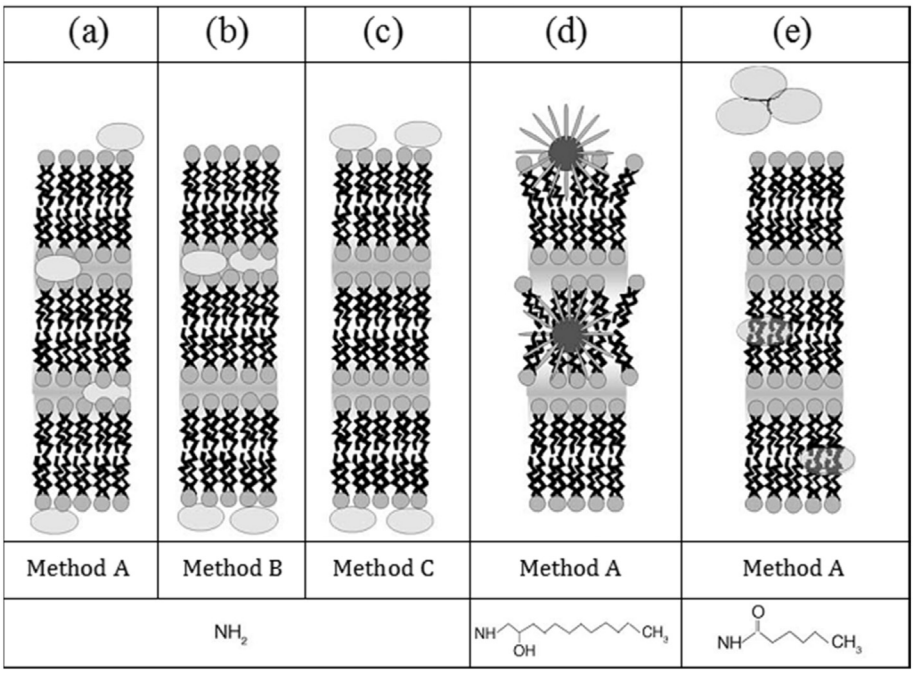

Fig. 6. Proposed model for interactions between MLVs and G3 PAMAM dendrimers with different functionalisation. Combining G3 dendrimers with lipids at different stages in MLV production resulted in differences in the thermotropic behaviour of the liposomes, measured using DSC. Amine terminated dendrimers added during the production of a lipid film *before* hydration (Method A; a), were uniformly distributed throughout the vesicles, resulting in a symmetrical DSC transition peak. Amine terminated dendrimers added *during* the hydration of the film (Method B; b) and to pre-formed MLV vesicles (Method C; c) produced asymmetrical transition peaks, indicative of less dendrimer penetration through the membranes. Dendrimers with 50% hydrophobic C_{12} groups on the periphery (d) were found to cause more disruption to the vesicle membranes, whereas dendrimers with hydrophobic hexylamide terminations (e) had weaker interactions with the membrane due to aggregation of the dendrimers. Adapted from [114] copyright 2005, with permission from Elsevier.

liposomes' size, shape, periodicity, charge and contents leakage have been measured in the presence of varying concentration, size and charge of PAMAM dendrimers. Energetic changes in the liposomes liquid-crystalline transitions in the presence of dendrimers was also studied using DSC. These studies have been able to elude to how the physicochemical properties of dendrimers, including surface functionality and size, have affected their interactions with lipid vesicles of varying composition and lamellarity. The charge of the dendrimers and composition of the liposomal membranes was found to play a major role in these interactions. The functionalisation of the dendrimer has been found to change its overall shape and rigidity, which in turn influences its interactions with a flexible membrane. The amine-terminated dendrimers can deform against a bilayer or substrate as suggested by computational studies [116] and observed through AFM [117, 118], reducing the structural disruption of the bilayer.

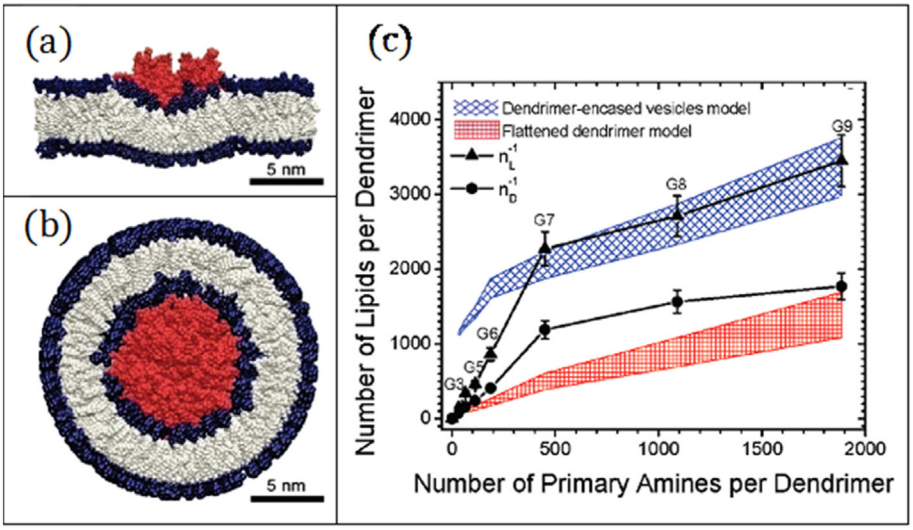

Fig. 7. (a) Flattened dendrimer model, and (b) dendrimer-encased vesicle model of dendrimer-lipid complexes. Larger dendrimers (>G6) were encased by lipids, whereas smaller dendrimers deformed against the bilayer and promoted membrane curvature. G5 and G7 are coloured red, the hydrophilic headgroups blue, and the hydrophobic tails grey. (c) ITC-determined binding stoichiometries for the dendrimer-lipid complexes compared with the expected stoichiometry of these models. Adapted with permission from [113]. Copyright 2009 American Chemical Society.

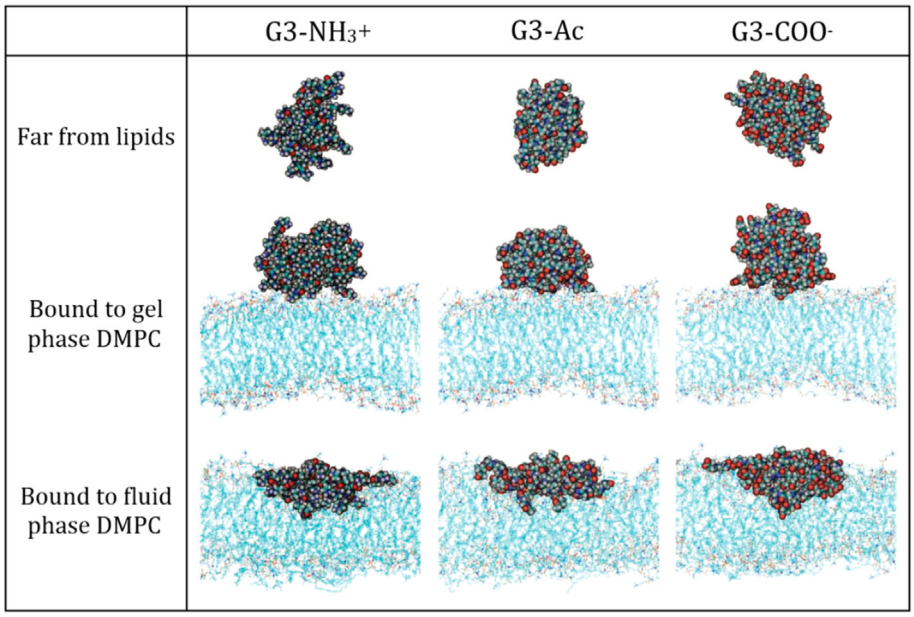

Fig. 8. Snapshots of atomistic MD simulations between DMPC bilayers and G3 PAMAM with various terminal groups including protonated amine (G3-NH_3^+), neutral acetamide (G3-Ac), and deprotonated carboxylic acid (G3-COO^-). The simulations reveal the differences in the morphologies of dendrimers interacting with either gel or fluid phase bilayers. Adapted with permission from Kelly et al. Copyright 2008 American Chemical Society.

4.4. Simulation studies on interactions between PAMAM dendrimers and model membranes

Computational simulations can contribute to understanding the complex dynamics and energetics during membrane penetration and endocytosis, with high spatial and temporal resolution, although it remains a significant challenge to construct realistic models and simulate endocytosis on a realistic timescale and with sub-molecular resolution. For example, molecular dynamics (MD) simulations can calculate precise mechanistic details from several angstroms to hundreds of nanometres. The model is defined by a force-field that describes electrostatic, van der Waals and bond interactions for an all atom or a coarse-grained (CG) model. However, the former is computationally expensive and time consuming, whereas CG simulations cluster atoms and molecules into beads to reduce computational demand. For example, a lipid molecule can be divided into 3 beads or into membrane 'units' to model interactions with larger particles. The system is virtually reproduced, considering many physical and chemical parameters. Mechanistic information, such as dendrimer penetration and pore formation, can be obtained from atomistic models alongside quantitative free energy calculations. Coarse-grained models can be used to explore the wrapping of the bilayer around dendrimers, or the translocation of dendrimers through the membrane. Lee and Larson provided a review of several computational models of interactions between dendrimers and bilayers or polyelectrolytes [119]. Here we will discuss the important results from those studies and several more recent examples.

4.4.1. Atomistic simulations

In 2005, Maiti et al. [120] ran atomistic simulations of G4–6 PAMAM dendrimers in water to calculate their radius of gyration. They also studied the effect of pH on water diffusion around the dendrimer and its effect on binding to other molecules. Mecke et al. [118] simulated interactions between PAMAM dendrimers and mica surfaces, finding the flattening of PAMAM dendrimers against mica, with the flattening being more profound with highly charged dendrimers. This flattening effect was described experimentally by Hong et al. [65] and was discussed in Section 4.1.

Kelly et al. [116] used atomistic MD simulations, alongside experiments discussed in 4.3, to investigate the molecular structures of PAMAM dendrimers binding to DMPC bilayers with three different terminations: protonated amine, neutral acetamide, and deprotonated carboxylic acid (Fig. 8). They also investigated the effect of the liquid-crystalline phase of the lipid bilayer (fluid or gel) on the binding of G3 dendrimers, relevant to endocytosis mechanisms, lipid removal and the formation of membrane pores. Dendrimers bound to the fluid phases kept their spherical shape, whereas dendrimers bound to the gel phases flattened and formed over twice as many dendrimer-lipid contacts. All terminations of dendrimers also intercalated into the bilayer in the fluid phase, but not in gel phase. The lipids in the fluid phases rearranged so that the hydrophobic regions of the dendrimer could be accessed by the lipid tails and the polar dendrimer regions had polar lipid headgroups nearby. Dendrimer binding to fluid over gel phases was found to be influenced by the inner dendrimer structure rather than the termination. This was interesting as several experimental studies found differences in interactions between dendrimers and SLBs in different crystalline phases [65, 88, 98].

Kim et al. [121] used atomistic models to study the interactions between a G3 PAMAM dendrimer and both zwitterionic (DPPC) and anionic (POPG) bilayer membranes. Van der Waals interactions were dominant for the DPPC membrane interactions. Electrostatic interactions pulled the G3 dendrimer into the headgroup region of the POPG bilayer, causing perturbation in the membrane and the dendrimer to change shape and flatten against the bilayer. However, this model did not consider the curvature of the membrane induced by the change in surface tension of the membrane leaflets by incorporation of the dendrimer.

4.4.2. Coarse-grained simulations

A CG model was developed for cationic and neutral G3–7 PAMAM dendrimers by Lee and Larson in 2006, [122] so that multiple dendrimers could be simulated interacting with lipid bilayers. Simulations using these models interacting with DMPC bilayers found that cationic G5 and G7 dendrimers caused pore

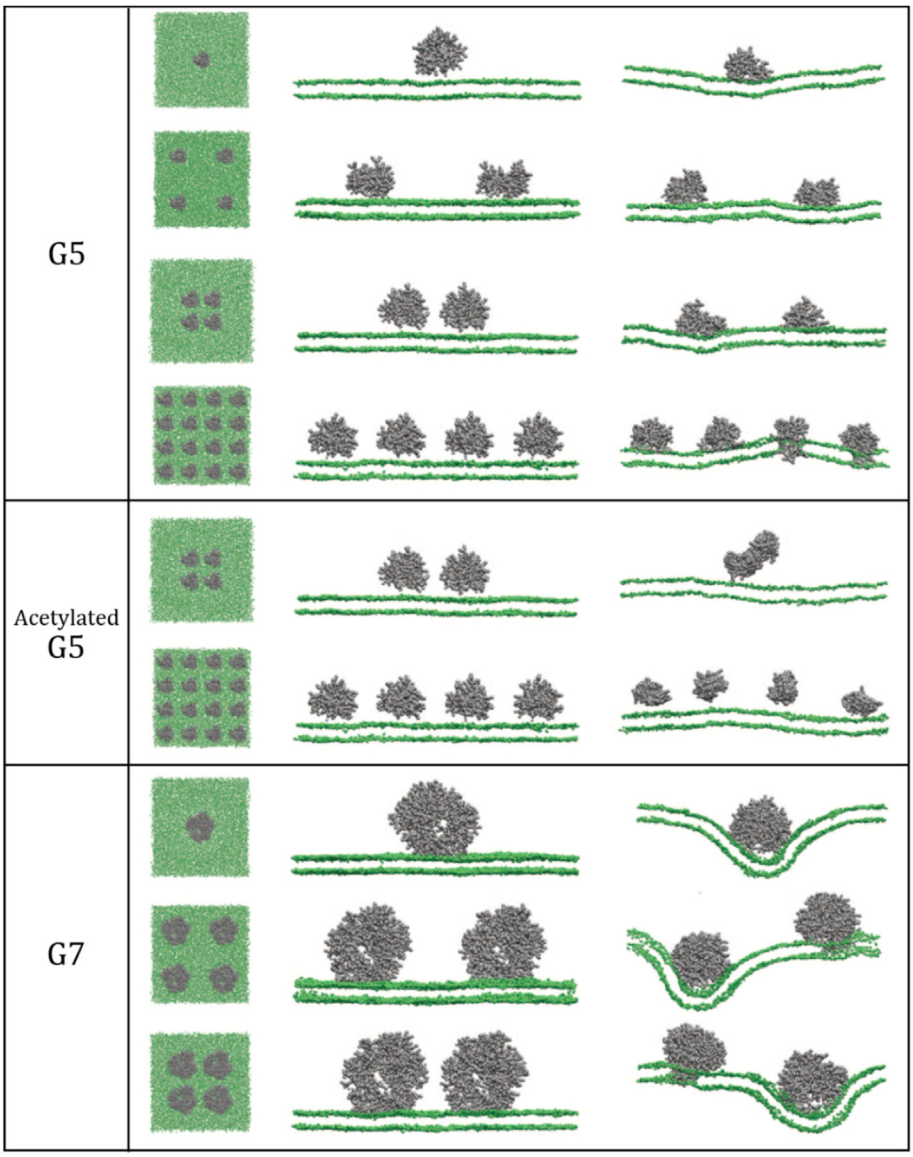

Fig. 9. Snapshots of a top view and side view during MD simulations of DMPC bilayers and G5 and G7 dendrimers, both acetylated and un-acetylated and at varying density. Grey dots represent dendrimers and green dots represent the headgroups of the DMPC bilayer. Un-acetylated dendrimers that were initially clustered together did not aggregate and instead repelled each other due to the repulsive interactions between their terminal groups. High generation dendrimers were found to cause pore formation due to significant bending of the membrane. The pore formation was dependent upon the generation and the number of dendrimers present on the membrane. Reprinted with permission from [122]. Copyright 2006 American Chemical Society.

formation whereas neutral dendrimers did not. The effects of dendrimer clustering, concentration and acetylation on DMPC bilayers [123] were also studied, and snapshots of these simulations are shown in Fig. 9. The higher charge densities of high generation NH_2-terminated dendrimers initiated pore formation, whereas neutral dendrimers were found to cluster together and did not form pores. This correlates with pore formation caused by high generation dendrimers in SLBs as discussed in Section 4.1.

Tian and Ma [124] used CG simulations to study the effect of pH on the interactions between G2–4 PAMAM dendrimers and DPPG:DPPC (1:3) bilayers. G4 was found to adsorb to membranes in physiological conditions and cause pore formation and the formation of an asymmetric bilayer in acidic conditions. Lin et al. [125] used CG MD simulations to study G3, G5 and G7 neutral PAMAM dendrimers interacting with a zwitterionic DPPC monolayer. Both G5 and G7 had structural effects of the monolayer. When compressed, DPPC formed microdomains of a gel phase, and interfacial molecules went from a coexisting phase liquid-expanded (LE) and liquid-condensed (LC) to a pure LC phase. However, with the addition of neutral G5 or G7 PAMAM dendrimers this phase transition was supressed or reversed. These results correlate well with the monolayer experimental studies discussed in Section 4.2, showing changes in molecular packing in the presence of PAMAM dendrimers.

The interactions between cationic G4 and G5 PAMAM dendrimers and asymmetric DPPC/DPPE/DPPS membranes have also been studied by He et al. using CG simulations [126]. When the outer leaflet of the membrane contained 10% DPPS and the inner leaflet contained 50% DPPS, it was found that the G4 dendrimer inserted into the outer membrane and the G5 dendrimer caused pore formation. Both generations of dendrimer only adsorbed to the inner side of the membrane. As the asymmetry of the membrane increased, the G4 dendrimer could penetrate further into the membrane. At 50% DPPS the G4 dendrimer could translocate from the outer to the inner leaflet. This study highlights

the impact of membrane asymmetry, which is found in most cellular membranes, on interactions between bilayers and dendrimers. It also highlights the ability of dendrimers to translocate passively through cellular membranes, as observed by several others experimentally [14, 57, 85].

5. Summary and outlook

The precise control over PAMAM dendrimers physicochemical properties including size and surface functionality have made them ideal candidates for a range of biomedical applications from imaging agents to gene transfection vectors. However, uncertainties in the effect of these properties on the cytotoxicity and endocytosis mechanisms have hindered this progress. Model membranes such as supported lipid bilayers, Langmuir monolayers and liposomes have been used to as model membranes to study their interactions with PAMAM dendrimers using a range of rigorous physical techniques. By varying the composition, and hence charge and phase behaviour, different cellular membrane systems have been modelled. PAMAM dendrimers have been found to alter the structural properties of lipid membranes in a size, charge and concentration dependant manner. High generation dendrimers (>G4) can cause pore formation and strip lipids from the membranes, whereas low generation dendrimers (<G5) have been found to intercalate or adsorb to membrane surfaces. These interactions are further governed by electrostatic interactions between cationic or anionic terminated dendrimers and charged membrane lipids, with charge-terminated dendrimers resulting in greater disruption to the membranes than neutral dendrimers. Disruption in membrane packing and pore formation has also been shown to vary with concentration. The presence of large numbers of dendrimers increases the number of dendrimer-lipid interactions, while decreasing the number of lipid-lipid interactions, leading to de-stability. The effect of steric crowing of surface groups on high generation dendrimers made them rigid and less deformable than lower generation dendrimers. Low generation dendrimers have been found to deform against the membrane, flattening and increasing the number of charge-charge interactions whereas the inflexibility and high charge density of high generation dendrimers resulted in increased membrane curvature.

Future challenges include the extension of these membrane models to better represent living systems and become more biologically relevant. These membrane models have also focussed on the effect of PAMAM physicochemical properties on the physical structure of, and insertion into, cellular membranes. Further questions have arisen from these studies and are yet to be answered. For example, how do PAMAM improve DNA transfection and what are the mechanisms involved? Initially, this has been shown to be influenced by the ratio of PAMAM dendrimer terminal amine groups to DNA groups. Furthermore, the energetic barriers involved in phase transitions have shown to be influenced by PAMAM dendrimers, but the dendrimers' role remains unclear. Many groups have measured changes to the fluidity of the acyl chain region, but it remains unclear where the dendrimers are located within the bilayers. Interactions between lipid mesophases and PAMAM dendrimers, measured using SAXS, may be able to elude to an answer. By studying the change in transition temperature or pressure as a function of dendrimer concentration, this energetic change may be better understood. The molecular deformations involved in membrane fusion are identical to those found in these mesophase transitions and further study on this may also be able to give physical insight into endocytosis mechanisms. Finding the location of dendrimers within these model bilayers by use of freeze fracture TEM or confocal microscopy may help to give conformation of the positioning of these dendrimers within bilayers. An understanding of how dendrimer physicochemical properties influence interactions with cells could pave the way for intelligent drug carrier design, improving the effectiveness and specificity of drugs.

Acknowledgements

We acknowledge funding from the Engineering and Physical Science Research Council (EPSRC EP/L016648/1 through the Bristol Centre for Functional Nanomaterials (BCFN) and EP/H034862/1).

List of abbreviations

PAMAM	polyamidoamine
G1, G2 …	generation 1, generation 2 …
SLB	supported lipid bilayer
MLV	multi-lamellar vesicle
SUV	small unilamellar vesicle
LUV	large unilamellar vesicle
GUV	giant unilamellar vesicle
ROS	reactive oxygen species
TUNEL	terminal deoxynucleotidyl transferase (TdT) dUTP nick-End labeling
MTT	3-(4,5-dimethylthiazol-2-yl)-2,5-diphenyltetrazolium bromidefor
LDH	lactate dehydrogenase
Luc	luciferace
MIP-2	mouse macrophage inflammatory protein 2
IL-6	interleukin-6
TNF-α	tumor necrosis factor alpha
ABTS	2,2′-azino-bis(3-ethylbenzothiazoline-6-sulphonic acid)
DCF	2′,7′-dichlorofluorescein
FACS	fluorescence activated cell sorting
RT-PCR	reverse transcription polymerase chain reaction
AO/EB	acridine orange/ethidium bromide
PE	phosphatidylethanolamine
PS	phosphatidylserine
PC	phosphatidylcholine
PA	phosphatidic acid
PG	phosphatidylglycerol
PI	phosphatidylinositol
DOPC	1,2-dioleoyl-sn-glycero-3-phosphocholine
DOPE	1,2-dioleoyl-sn-glycero-3-phosphoethanolamine
DPPC	1,2-dipalmitoyl-sn-glycero-3-phosphocholine
DPPS	1,2-dipalmitoyl-sn-glycero-3-phosphoserine
DPPC-d62	1,2-dipalmitoyl-d62-sn-glycero-3-phosphocholine
DPPG	1,2-dipalmitoyl-sn-glycero-3-phospho-(1′-rac-glycerol)
DMPC	1,2-dimyristoyl-sn-glycero-3-phosphocholine
DMPG	1,2-dimyristoyl-sn-glycero-3-phospho-(1′-rac-glycerol)
POPC	1-palmitoyl-2-oleoyl-sn-glycero-3-phosphocholine
POPA	1-palmitoyl-2-oleoyl-sn-glycero-3-phosphate
POPE	1-palmitoyl-2-oleoyl-sn-glycero-3-phosphoethanolamine
POPG	1-palmitoyl-2-oleoyl-sn-glycero-3-phospho-(1′-rac-glycerol)
AFM	atomic force microscopy
DLS	dynamic light scattering
XRR	X-ray reflectivity
NR	neutron reflectivity
QCM-D	quartz crystal microbalance with dissipation monitoring
DSC	differential scanning calorimetry
BAM	Brewster angle microscopy
SAXS/WAXS	small angle X-ray scattering/wide angle X-ray scattering
^{31}P NMR	phosphorus-31 nuclear magnetic resonance
MD	molecular dynamics
CG	coarse-grained
Cryo-TEM	cryogenic transmission electron microscopy
SWCNT	single walled carbon nanotubes
MWCNT	multi walled carbon nanotubes

References

[1] Pumera M, et al. Electrochemical nanobiosensors. Sens Actuat B Chem 2007;123(2):1195–205.
[2] Chaudhry Q, et al. Applications and implications of nanotechnologies for the food sector. Food Addit Contam Part A Chem Anal Control Expo Risk Assess 2008;25(3):241–58.
[3] Pilkington GA, Briscoe WH. Nanofluids mediating surface forces. Adv Colloid Interface Sci 2012;179:68–84.
[4] Conner SD, Schmid SL. Regulated portals of entry into the cell. Nature 2003;422:37.
[5] Nel AE, et al. Understanding biophysicochemical interactions at the nano-bio interface. Nat Mater 2009;8(7):543–57.
[6] Beddoes CM, Case CP, Briscoe WH. Understanding nanoparticle cellular entry: A physicochemical perspective. Adv Colloid Interface Sci 2015;218:48–68.

[7] Pourianazar NT, Mutlu P, Gunduz U. Bioapplications of poly(amidoamine) (PAMAM) dendrimers in nanomedicine. J Nanopart Res 2014:**16**(4).
[8] Gardikis K, et al. Dendrimers and the development of new complex nanomaterials for biomedical applications. Curr Med Chem 2012;19(29):4913–28.
[9] Markatou E, et al. Molecular interactions between dimethoxycurcumin and Pamam dendrimer carriers. Int J Pharm 2007;339(1–2):231–6.
[10] Yu GS, et al. Synthesis of PAMAM dendrimer derivatives with enhanced buffering capacity and remarkable gene transfection efficiency. Bioconjug Chem 2011;22 (6):1046–55.
[11] Mukherjee SP, Davoren M, Byrne HJ. In vitro mammalian cytotoxicological study of PAMAM dendrimers - towards quantitative structure activity relationships. Toxicol In Vitro 2010;24(1):169–77.
[12] Mukherjee SP, et al. Mechanistic studies of in vitro cytotoxicity of poly(amidoamine) dendrimers in mammalian cells. Toxicol Appl Pharmacol 2010;248(3): 259–68.
[13] Navarro G, Tros de Ilarduya C. Activated and non-activated PAMAM dendrimers for gene delivery in vitro and in vivo. Nanomedicine 2009;5(3):287–97.
[14] Ainalem ML, et al. On the ability of PAMAM dendrimers and dendrimer/DNA aggregates to penetrate POPC model biomembranes. J Phys Chem B 2010;114(21): 7229–44.
[15] Kulthe SS, et al. Polymeric micelles: Authoritative aspects for drug delivery. Design Monom Polym 2012;15(5):465–521.
[16] Elsabahy M, Wooley KL. Design of polymeric nanoparticles for biomedical delivery applications. Chem Soc Rev 2012;41(7):2545–61.
[17] Scott RW, Wilson OM, Crooks RM. Synthesis, characterization, and applications of dendrimer-encapsulated nanoparticles. J Phys Chem B 2005;109(2):692–704.
[18] Majoral JP, Caminade AM. Dendrimers containing heteroatoms (si, p, B, ge, or bi). Chem Rev 1999;99(3):845–80.
[19] Jiang YH, et al. SPL7013 gel as a topical microbicide for prevention of vaginal transmission of SHIV89.6P in macaques. AIDS Res Hum Retroviruses 2005;21(3): 207–13.
[20] Jackson CL, et al. Visualization of dendrimer molecules by transmission electron microscopy (TEM): Staining methods and Cryo-TEM of vitrified solutions. Macromolecules 1998;31(18):6259–65.
[21] Dobrovolskaia MA, et al. Nanoparticle size and surface charge determine effects of PAMAM dendrimers on human platelets in vitro. Mol Pharm 2012;9(3):382–93.
[22] Muller R, et al. Determination of molecular weight, particle size, and density of high number generation PAMAM dendrimers using MALDI-TOF-MS and nES-GEMMA. Macromolecules 2007;40(15):5599–605.
[23] Prosa TJ, et al. A SAXS study of the internal structure of dendritic polymer systems. J Polym Sci Part B Polym Phys 1997;35(17):2913–24.
[24] Maiti PK, et al. Structure of PAMAM dendrimers: Generations 1 through 11. Macromolecules 2004;37(16):6236–54.
[25] Tomalia DA, et al. A new class of polymers - starburst-dendritic macromolecules. Polym J 1985;17(1):117–32.
[26] Wang B, et al. Inhibition of bacterial growth and intramniotic infection in a Guinea pig model of chorioamnionitis using PAMAM dendrimers. Int J Pharm 2010;395(1–2):298–308.
[27] Luong D, et al. PEGylated PAMAM dendrimers: Enhancing efficacy and mitigating toxicity for effective anticancer drug and gene delivery. Acta Biomater 2016;43: 14–29.
[28] Tomalia DA. Starburst dendrimers - molecular-level control of size, shape, surface-chemistry, topology, and flexibility from atoms to macroscopic matter. Abst Papers Am Chem Soc 1990;**199** (p. 315-Orgn).
[29] Choudhary S, et al. Impact of dendrimers on solubility of hydrophobic drug molecules. Front Pharmacol 2017;8:261.
[30] Pilkington GA, Pedersen JS, Briscoe WH. Dendrimer nanofluids in the concentrated regime: From polymer melts to soft spheres. Langmuir 2015;31(11): 3333–42.
[31] Tomalia DA, Naylor AM, Goddard WA. Starburst dendrimers: Molecular-level control of size, shape, surface chemistry, topology, and flexibility from atoms to macroscopic matter. Angew Chem Int Edn English 1990;29(2):138–75.
[32] Twyman LJ, et al. The synthesis of water soluble dendrimers, and their application as possible drug delivery systems. Tetrahedron Lett 1999;40(9):1743–6.
[33] Konda SD, et al. Specific targeting of folate-dendrimer MRI contrast agents to the high affinity fo late receptor expressed in ovarian tumor xenografts. Magn Reson Mater Phys Bio Med 2001;12(2–3):104–13.
[34] Bezouška K. Design, functional evaluation and biomedical applications of carbohydrate dendrimers (glycodendrimers). Rev Mol Biotechnol 2002;90(3–4):269–90.
[35] Haensler J, Szoka Jr FC. Polyamidoamine cascade polymers mediate efficient transfection of cells in culture. Bioconjug Chem 1993;4(5):372–9.
[36] Eichman JD, et al. The use of PAMAM dendrimers in the efficient transfer of genetic material into cells. Pharmaceut Sci Technol Today 2000;3(7):232–45.
[37] Kesharwani P, et al. PAMAM dendrimers as promising nanocarriers for RNAi therapeutics. Mater Today 2015;18(10):565–72.
[38] Liu X, et al. Structurally flexible triethanolamine core PAMAM dendrimers are effective nanovectors for DNA transfection in vitro and in vivo to the mouse thymus. Bioconjug Chem 2011;22(12):2461–73.
[39] Arima H, et al. Enhancement of gene expression by polyamidoamine dendrimer conjugates with alpha-, beta-, and gamma-cyclodextrins. Bioconjug Chem 2001; 12(4):476–84.
[40] Yoo H, Juliano RL. Enhanced delivery of antisense oligonucleotides with fluorophore-conjugated PAMAM dendrimers. Nucleic Acids Res 2000;28(21): 4225–31.
[41] Pavan GM, et al. PAMAM dendrimers for siRNA delivery: Computational and experimental insights. Chem A Eur J 2010;16(26):7781–95.
[42] Mandal T, Kumar MVS, Maiti PK. DNA assisted self-assembly of PAMAM dendrimers. J Phys Chem B 2014;118(40):11805–15.
[43] Conti DS, et al. Poly(amidoamine) dendrimer nanocarriers and their aerosol formulations for siRNA delivery to the lung epithelium. Mol Pharm 2014;11(6):1808–22.
[44] Langereis S, et al. Dendrimers and magnetic resonance imaging. New J Chem 2007; 31(7):1152–60.
[45] Longmire M, Choyke PL, Kobayashi H. Dendrimer-based contrast agents for molecular imaging. Curr Top Med Chem 2008;8(14):1180–6.
[46] Wiener EC, et al. Molecular dynamics of ion-chelate complexes attached to dendrimers. J Am Chem Soc 1996;118(33):7774–82.
[47] Bryant Jr LH, et al. Synthesis and relaxometry of high-generation (G = 5, 7, 9, and 10) PAMAM dendrimer-DOTA-gadolinium chelates. J Magn Reson Imaging 1999;9 (2):348–52.
[48] Mekuria SL, Debele TA, Tsai HC. Encapsulation of gadolinium oxide nanoparticle (Gd2O3) contrasting agents in PAMAM dendrimer templates for enhanced magnetic resonance imaging in vivo. ACS Appl Mater Interfaces 2017;9(8):6782–95.
[49] Opina AC, et al. Preparation and long-term biodistribution studies of a PAMAM dendrimer G5-Gd-BnDOTA conjugate for lymphatic imaging. Nanomedicine (Lond) 2015;10(9):1423–37.
[50] Islas L, et al. Singly and binary grafted poly(vinyl chloride) urinary catheters that elute ciprofloxacin and prevent bacteria adhesion. Int J Pharm 2015;488(1–2): 20–8.
[51] Calabretta MK, et al. Antibacterial activities of poly(amidoamine) dendrimers terminated with amino and poly(ethylene glycol) groups. Biomacromolecules 2007; 8(6):1807–11.
[52] Lopez AI, et al. Antibacterial activity and cytotoxicity of PEGylated poly(amidoamine) dendrimers. Mol Biosyst 2009;5(10):1148–56.
[53] Albertazzi L, et al. Dendrimer internalization and intracellular trafficking in living cells. Mol Pharm 2010;7(3):680–8.
[54] Perumal OP, et al. The effect of surface functionality on cellular trafficking of dendrimers. Biomaterials 2008;29(24):3469–76.
[55] Kitchens KM, et al. Endocytosis and interaction of poly (amidoamine) dendrimers with Caco-2 cells. Pharm Res 2007;24(11):2138–45.
[56] El-Sayed M, et al. Transepithelial transport of poly(amidoamine) dendrimers across Caco-2 cell monolayers. J Control Release 2002;81(3):355–65.
[57] Maher MA, Byrne HJ. Modification of the in vitro uptake mechanism and antioxidant levels in HaCaT cells and resultant changes to toxicity and oxidative stress of G4 and G6 poly(amidoamine) dendrimer nanoparticles. Anal Bioanal Chem 2016;408(19):5295–307.
[58] Manunta M, et al. Gene delivery by dendrimers operates via a cholesterol dependent pathway. Nucleic Acids Res 2004;32(9):2730–9.
[59] Svenson S, Tomalia DA. Dendrimers in biomedical applications—reflections on the field. Adv Drug Deliv Rev 2005;57(15):2106–29.
[60] Naha PC, et al. Reactive oxygen species (ROS) induced cytokine production and cytotoxicity of PAMAM dendrimers in J774A.1 cells. Toxicol Appl Pharmacol 2010; 246(1–2):91–9.
[61] Albertazzi L, et al. In vivo distribution and toxicity of PAMAM dendrimers in the central nervous system depend on their surface chemistry. Mol Pharm 2013;10 (1):249–60.
[62] Janaszewska A, et al. Cytotoxicity of PAMAM, PPI and maltose modified PPI dendrimers in Chinese hamster ovary (CHO) and human ovarian carcinoma (SKOV3) cells. New J Chem 2012;36(2):428–37.
[63] Lee JH, et al. Nanosized polyamidoamine (PAMAM) dendrimer-induced apoptosis mediated by mitochondrial dysfunction. Toxicol Lett 2009;190(2):202–7.
[64] Halets I, et al. Contribution of hydrophobicity, DNA and proteins to the cytotoxicity of cationic PAMAM dendrimers. Int J Pharm 2013;454(1):1–3.
[65] Hong S, et al. Interaction of poly(amidoamine) dendrimers with supported lipid bilayers and cells: Hole formation and the relation to transport. Bioconjug Chem 2004;15(4):774–82.
[66] Janaszewska A, et al. Modified PAMAM dendrimer with 4-carbomethoxypyrrolidone surface groups reveals negligible toxicity against three rodent cell-lines. Nanomedicine 2013;9(4):461–4.
[67] Santos JL, et al. Functionalization of poly(amidoamine) dendrimers with hydrophobic chains for improved gene delivery in mesenchymal stem cells. J Control Release 2010;144(1):55–64.
[68] Ciolkowski M, et al. The influence of PAMAM dendrimers surface groups on their interaction with porcine pepsin. Biochim Biophys Acta 2013;1834(10):1982–7.
[69] Vidal F, Guzman L. Dendrimer nanocarriers drug action: Perspective for neuronal pharmacology. Neural Regen Res 2015;10(7):1029–31.
[70] Kannan RM, Perumal OP, Kannan S. Dendrimers and hyperbranched polymers for drug delivery. In: Labhasetwar VAL-P, editor. Biomedical Applications of Nanotechnology. Wiley; 2007. p. 105.
[71] Rascol E, Devoisselle JM, Chopineau J. The relevance of membrane models to understand nanoparticles-cell membrane interactions. Nanoscale 2016;8(9): 4780–98.
[72] Langmuir I. The mechanism of the surface phenomena of flotation. Trans Faraday Soc 1920;15(3):0062–74.
[73] Langmuir I, Blodgett KB. Regarding some new methods for the investigation of monomolecular layers. Kolloid-Zeitschrift 1935;73(3):257–63.
[74] Blodgett KB. Films built by depositing successive monomolecular layers on a solid surface. J Am Chem Soc 1935;57(1):1007–22.
[75] Bulpett JM, et al. Hydrophobic nanoparticles promote lamellar to inverted hexagonal transition in phospholipid mesophases. Soft Matter 2015;11(45):8789–800.
[76] Beddoes CM, et al. Hydrophilic nanoparticles stabilising mesophase curvature at low concentration but disrupting mesophase order at higher concentrations. Soft Matter 2016;12(28):6049–57.

[77] Tamm LK, McConnell HM. Supported phospholipid-bilayers. Biophys J 1985;47(1):105–13.
[78] Eytan GD. Use of liposomes for reconstitution of biological functions. Biochim Biophys Acta 1982;694(2):185–202.
[79] Kox AJ, Michels JPJ, Wiegel FW. Simulation of a lipid monolayer using molecular-dynamics. Nature 1980;287(5780):317–9.
[80] Sironi B, et al. Structure of lipid multilayers via drop casting of aqueous liposome dispersions. Soft Matter 2016;12(17):3877–87.
[81] Akesson A, et al. Unraveling dendrimer translocation across cell membrane mimics. Langmuir 2012;28(36):13025–33.
[82] Leroueil PR, et al. Nanoparticle interaction with biological membranes: Does nanotechnology present a Janus face? Acc Chem Res 2007;40(5):335–42.
[83] Attwood SJ, Choi Y, Leonenko Z. Preparation of DOPC and DPPC supported planar lipid bilayers for atomic force microscopy and atomic force spectroscopy. Int J Mol Sci 2013;14(2):3514–39.
[84] Mecke A, et al. Direct observation of lipid bilayer disruption by poly(amidoamine) dendrimers. Chem Phys Lipids 2004;132(1):3–14.
[85] Yanez Arteta M, et al. Interactions of PAMAM dendrimers with negatively charged model biomembranes. J Phys Chem B 2014;118(45):12892–906.
[86] Bailey CM, et al. Size dependence of gold nanoparticle interactions with a supported lipid bilayer: A QCM-D study. Biophys Chem 2015;203-204:51–61.
[87] Smith PE, et al. Solid-state NMR reveals the hydrophobic-core location of poly(amidoamine) dendrimers in biomembranes. J Am Chem Soc 2010;132(23):8087–97.
[88] Gardikis K, et al. A DSC and Raman spectroscopy study on the effect of PAMAM dendrimer on DPPC model lipid membranes. Int J Pharm 2006;318(1–2):118–23.
[89] Anderson TH, et al. Formation of supported bilayers on silica substrates. Langmuir 2009;25(12):6997–7005.
[90] Richter RP, Brisson AR. Following the formation of supported lipid bilayers on mica: A study combining AFM, QCM-D, and ellipsometry. Biophys J 2005;88(5):3422–33.
[91] Richter RP, Berat R, Brisson AR. Formation of solid-supported lipid bilayers: An integrated view. Langmuir 2006;22(8):3497–505.
[92] Aeffner S, et al. Energetics of stalk intermediates in membrane fusion are controlled by lipid composition. Proc Natl Acad Sci U S A 2012;109(25):E1609–18.
[93] Keidel A, Bartsch TF, Florin EL. Direct observation of intermediate states in model membrane fusion. Sci Rep 2016;6:23691.
[94] Siegel DP, Epand RM. The mechanism of the lamellar/inverted hexagonal phase transition and its relationship to membrane fusion: Evidence from time-resolved cryoelectron microscopy, NMR and DSC. Biophys J 1997;**72**(2) (p. Wp303-Wp303).
[95] Lingwood D, Simons K. Lipid rafts as a membrane-organizing principle. Science 2010;327(5961):46–50.
[96] Mecke A, et al. Lipid bilayer disruption by polycationic polymers: The roles of size and chemical functional group. Langmuir 2005;21(23):10348–54.
[97] Parimi S, Barnes TJ, Prestidge CA. PAMAM dendrimer interactions with supported lipid bilayers: A kinetic and mechanistic investigation. Langmuir 2008;24(23):13532–9.
[98] Keszthelyi T, et al. Bilayer charge reversal and modification of lipid organization by dendrimers as observed by sum-frequency vibrational spectroscopy. Langmuir 2015;31(28):7815–25.
[99] Mecke A, et al. Synthetic and natural polycationic polymer nanoparticles interact selectively with fluid-phase domains of DMPC lipid bilayers. Langmuir 2005;21(19):8588–90.
[100] Girard-Egrot APAB. Langmuir-Blodgett technique for synthesis of biomimetic lipid membranes. In: Martin DK, editor. Nanobiotechnology of biomimetic membranes. New York: Springer; 2007. p. 23–74.
[101] Abraham N, et al. Interaction of biofunctionalized gold nanoparticles with model phospholipid membranes. Colloid Polym Sci 2014;292(10):2715–25.
[102] Guzman E, et al. Mixed DPPC-cholesterol Langmuir monolayers in presence of hydrophilic silica nanoparticles. Colloids Surf B Biointerfaces 2013;**105**(Supplement C):284–93.
[103] Knobloch J, et al. Membrane-drug interactions studied using model membrane systems. Saudi J Biol Sci 2015;22(6):714–8.
[104] Cancino J, et al. A new strategy to investigate the toxicity of nanomaterials using Langmuir monolayers as membrane models. Nanotoxicology 2013;7(1):61–70.
[105] Tiriveedhi V, et al. Kinetic analysis of the interaction between poly(amidoamine) dendrimers and model lipid membranes. Biochim Biophys Acta 2011;1808(1):209–18.
[106] Wilde M, et al. Biophysical studies in polymer therapeutics: The interactions of anionic and cationic PAMAM dendrimers with lipid monolayers. J Drug Target 2017;25(9–10):910–8.
[107] Lombardo D, et al. Effect of anionic and cationic polyamidoamine (PAMAM) dendrimers on a model lipid membrane. Biochim Biophys Acta 2016;1858(11):2769–77.
[108] Bangham AD, De Gier J, Greville GD. Osmotic properties and water permeability of phospholipid liquid crystals. Chem Phys Lipids 1967;1(3):225–46.
[109] Pattni BS, Chupin VV, Torchilin VP. New developments in liposomal drug delivery. Chem Rev 2015;115(19):10938–66.
[110] Berenyi S, et al. A mechanistic view of lipid membrane disrupting effect of PAMAM dendrimers. Colloids Surf B Biointerfaces 2014;118:164–71.
[111] Akesson A, et al. The effect of PAMAM G6 dendrimers on the structure of lipid vesicles. Phys Chem Chem Phys 2010;12(38):12267–72.
[112] Zhang ZY, Smith BD. High-generation polycationic dendrimers are unusually effective at disrupting anionic vesicles: Membrane bending model. Bioconjug Chem 2000;11(6):805–14.
[113] Kelly CV, et al. Stoichiometry and structure of poly(amidoamine) dendrimer-lipid complexes. ACS Nano 2009;3(7):1886–96.
[114] Klajnert B, Epand RM. PAMAM dendrimers and model membranes: Differential scanning calorimetry studies. Int J Pharm 2005;305(1–2):154–66.
[115] Karoonuthaisiri N, Titiyevskiy K, Thomas JL. Destabilization of fatty acid-containing liposomes by polyamidoamine dendrimers. Colloid Surfaces B Biointerf 2003;27(4):365–75.
[116] Kelly CV, et al. Poly(amidoamine) dendrimers on lipid bilayers II: Effects of bilayer phase and dendrimer termination. J Phys Chem B 2008;112(31):9346–53.
[117] Betley TA, et al. Tapping mode atomic force microscopy investigation of poly(amidoamine) dendrimers: Effects of substrate and pH on dendrimer deformation. Langmuir 2001;17(9):2768–73.
[118] Mecke A, et al. Deformability of poly(amidoamine) dendrimers. Eur Phys J E Soft Matter 2004;14(1):7–16.
[119] Lee H, Larson RG. Multiscale modeling of dendrimers and their interactions with bilayers and polyelectrolytes. Molecules 2009;14(1):423–38.
[120] Maiti PK, et al. Effect of solvent and pH on the structure of PAMAM dendrimers. Macromolecules 2005;38(3):979–91.
[121] Kim Y, Kwak Y, Chang R. Free energy of PAMAM dendrimer adsorption onto model biological membranes. J Phys Chem B 2014;118(24):6792–802.
[122] Lee H, Larson RG. Molecular dynamics simulations of PAMAM dendrimer-induced pore formation in DPPC bilayers with a coarse-grained model. J Phys Chem B 2006;110(37):18204–11.
[123] Lee H, Larson RG. Coarse-grained molecular dynamics studies of the concentration and size dependence of fifth- and seventh-generation PAMAM dendrimers on pore formation in DMPC bilayer. J Phys Chem B 2008;112(26):7778–84.
[124] Tian WD, Ma YQ. pH-responsive dendrimers interacting with lipid membranes. Soft Matter 2012;8(9):2627–32.
[125] Lin XB, Li Y, Gu N. Molecular dynamics simulations of the interactions of charge-neutral PAMAM dendrimers with pulmonary surfactant. Soft Matter 2011;7(8):3882–8.
[126] He X, et al. Molecular analysis of interactions between dendrimers and asymmetric membranes at different transport stages. Soft Matter 2014;10(1):139–48.